University of Stavanger

FACULTY OF SCIENCE AND TECHNOLOGY

Bachelor's Thesis

Study program/specialization: **Petroleum Engineering/ Drilling Technology**	Spring/Autumn semester, 2023 Open
Author: **Alexander Høyvik**	Alexander Høyvik ……. (Signature of author)
Program coordinator: Supervisor(s): **Mesfin Belayneh**	
Title of bachelor's thesis: ***Effect of SiO_2 nanoparticle and Quartz microparticle on the newly formulated geopolymer: Experimental and Modelling Studies*** Tittel på bacheloroppgave på norsk: ***Effekt av SiO_2 nanopartikler og Kvarts mikropartikler på den nylig formulerte geopolymeren: Eksperimentelle og modelleringsstudier***	
Credits: 20	
Keywords: Portland cement Geopolymer Quartz SiO_2 Nanoparticles Fly ash. Silicate Sodium hydroxide UCS	Number of pages: ……65…… + Supplemental material/other: 8 Date/year 15/05/2023 Stavanger

ACKNOWLEDGEMENTS

First and foremost, I would like to express my sincere gratitude to my supervisor, Mesfin Belayneh Agonafir, for his invaluable guidance and support throughout this thesis. His expertise, commitment to education, and unwavering dedication to his students have been a source of inspiration and motivation, for which I am truly grateful.

Secondly, I would like to extend my heartfelt appreciation to the University of Stavanger for allowing me to utilize their laboratory facilities and providing me with the necessary materials to conduct the experimental portion of this thesis. Their generosity and assistance have played a crucial role in the completion of my research.

Lastly, I would like to convey my deepest thanks to my family and friends for their unwavering encouragement and support throughout this semester. Their constant motivation and belief in my abilities have been the driving force behind my perseverance and success in this academic endeavor. It is with their love and support that I have been able to overcome challenges and complete the bachelor thesis.

ABSTRACT

In the oil and gas industry cement is used as a well barrier element. Well integrity studies on the North Sea production and injection wells have shown that about 11% of integrity failures are related to cement [6]. This is an indication that the oil well cement does not function without failure and hence does not satisfy the NORSOK D-10 standard requirements.

In recent years, the petroleum industry is searching for alternative materials for plug and abandonment operations. Among others, geopolymer is one of the candidates and it is currently under research phase. Before its application, geopolymers first should be qualified as a barrier element.

In this thesis, a new geopolymer was formulated and the impact of SiO_2 and quartz microparticles have also been investigated. The mechanical, rheological, and fluid leakage properties have been compared with the conventional properties of neat Portland G-class cement (OPC) after 10 days of curing (62ºC).

Results showed that:

- Newly formulated geopolymer improved uniaxial compressive strength and less fluid absorption compared to OPC.
- Minor changes with the addition of quartz and SiO_2 compared to the neat geopolymer reference.

These results are valid for the considered curing conditions like time, temperature, and pressure. Therefore, changing one or more of these may achieve different results.

TABLE OF CONTENTS

LIST OF FIGURES

LIST OF TABLES

LIST OF ABBREVIATIONS

API = American Petroleum Institute

HSR = High Sulphate Resistant

I.R = Insoluble Residue

ISO = International Organization for Standardization

MSR = Moderate Sulphate Resistant

NCS = Norwegian Continental Shelf

OPC = Ordinary Portland Cement

P&A = Plug and Abandonment

PSA = Petroleum Safety Authority

RPM = Revolution Per Minute

SEM = Scan Electron Microscope

UCS = Uniaxial Compressive Strength

WCR = Water to Cement Ratio

Wt% = Weight percent

%bwoc = Percent by weight of cement

LIST OF SYMBOLS

A = cross-sectional area of the specimen (mm^2)

E = Young´s modulus = (MPa)

Fmax = force at the time of failure (N)

G = Shear modulus (GPa)

K = Bulk modulus (GPa)

M = Modulus of Elasticity (GPa)

m = mass (g)

P = applied force at the moment the sample breaks (N)

Vp = Compressional wave velocity (km/s)

ρ = density (kg/m^3)

τ = Shear stress (Pa)

τ_c = Yield stress (Pa)

μ_c = Viscosity (Pa.s)

γ = Shear rate (sec^{-1})

ΔM = change of mass (%)

^oC = degrees Celsius

θ_{300} = 300RPM dial reading

1 INTRODUCTION

This BSc thesis presents the experimental and empirical modeling studies of a new geopolymer formulation and characterization. The neat geopolymer is synthesized by blending Fly ash and alkaline solutions (Sodium metasilicate and Sodium hydroxide). The effect of rock powder (Quartz) and silica nanoparticles on the neat geopolymer are also investigated. The geopolymer plugs were cured at 62ºC in the oven.

The characterization of geopolymer slurry and plugs were done through destructive tests (UCS and SEM) and Non-Destructive tests (Sonic, water absorption, leakage, and rheology). Using the destructive (UCS) and non-destructive (compressional wave velocity), an empirical model was developed. The model is trained and tested on the measured geopolymer dataset. Moreover, the model is compared with Shale rock and cement-based empirical models.

1.1 Background

During well construction, production and abandonment phases, cement is used as an important well barrier element. Well cementing can be classified into two operations: primary cementing and remedial cementing. Primary cementing involves placing cement around the casing to provide zonal isolation. The main functions are to prevent fluid migration in the annulus, support the casing or liner string, and protect the casing from corrosive formation fluids. [1]. On the other hand, in the event of a primary cementing failure, a remedial cementing operation is applied to repair the failed section through squeeze cementing or plug cementing. The latter are typically conducted when operators abandon a well when the productivity becomes uneconomical. [1]

Figure 1. 1 illustrates the typical cement placements of a final well structure. The application of cement on a plug and abandonment (P&A) well is also shown in Figure 1. 2. As seen, the cement plugs are placed as primary and secondary, used for flow zones or the reservoir, and surface plugs.

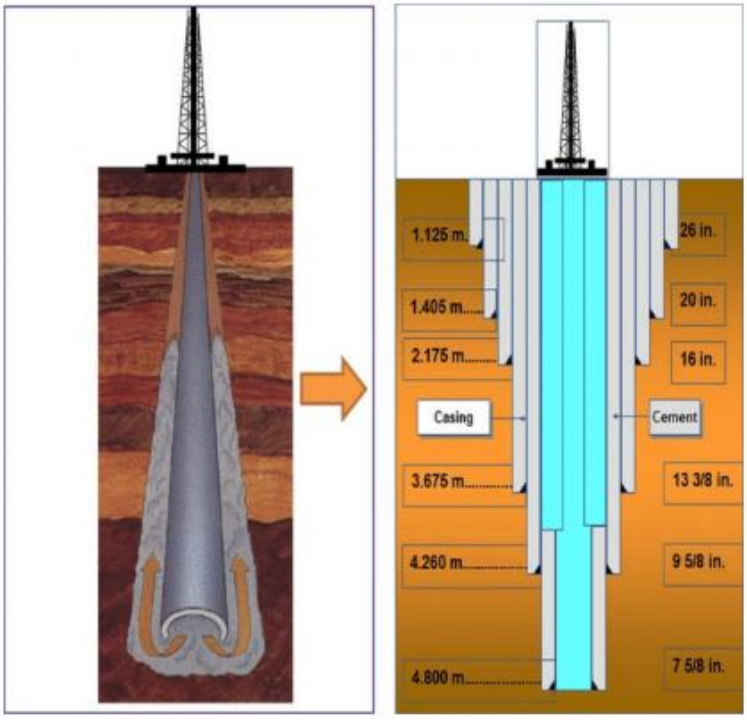

Figure 1. 1 Illustration of oil well cementing [2]

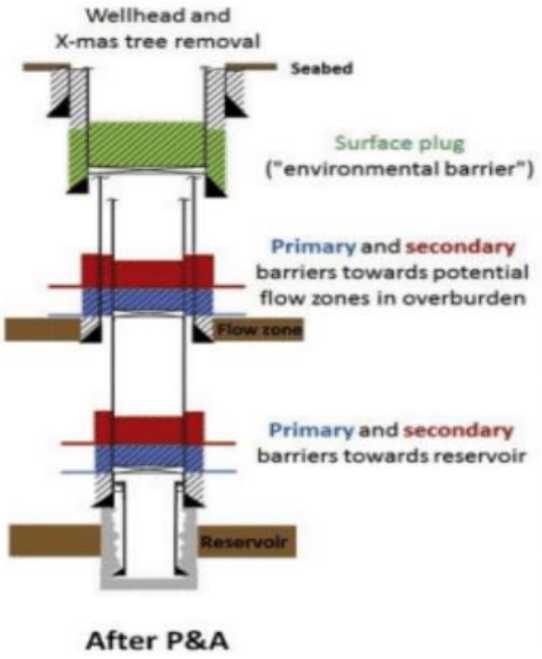

Figure 1. 2 Cement plug application for plug and abandonment operation [3]

A crucial factor to ensure a long-term integrity of the well, is good cement quality and a good cement job. However, over time, pressure and temperature loading could degrade the quality of cement by creating cracks, debonding, and shear failure mechanisms that will allow reservoir fluid leakage. The possible pathways for reservoir fluid to leak to the surface are shown below in Figure 1. 3. It can be observed that (a), (b), and (f) are leakage paths that likely are due to poor debonding between interfaces. Furthermore, (c) and (e) could originate from fractured

cement. The final leakage point (d) is a result of casing failure, for instance, due to corrosion or deformation. [4]

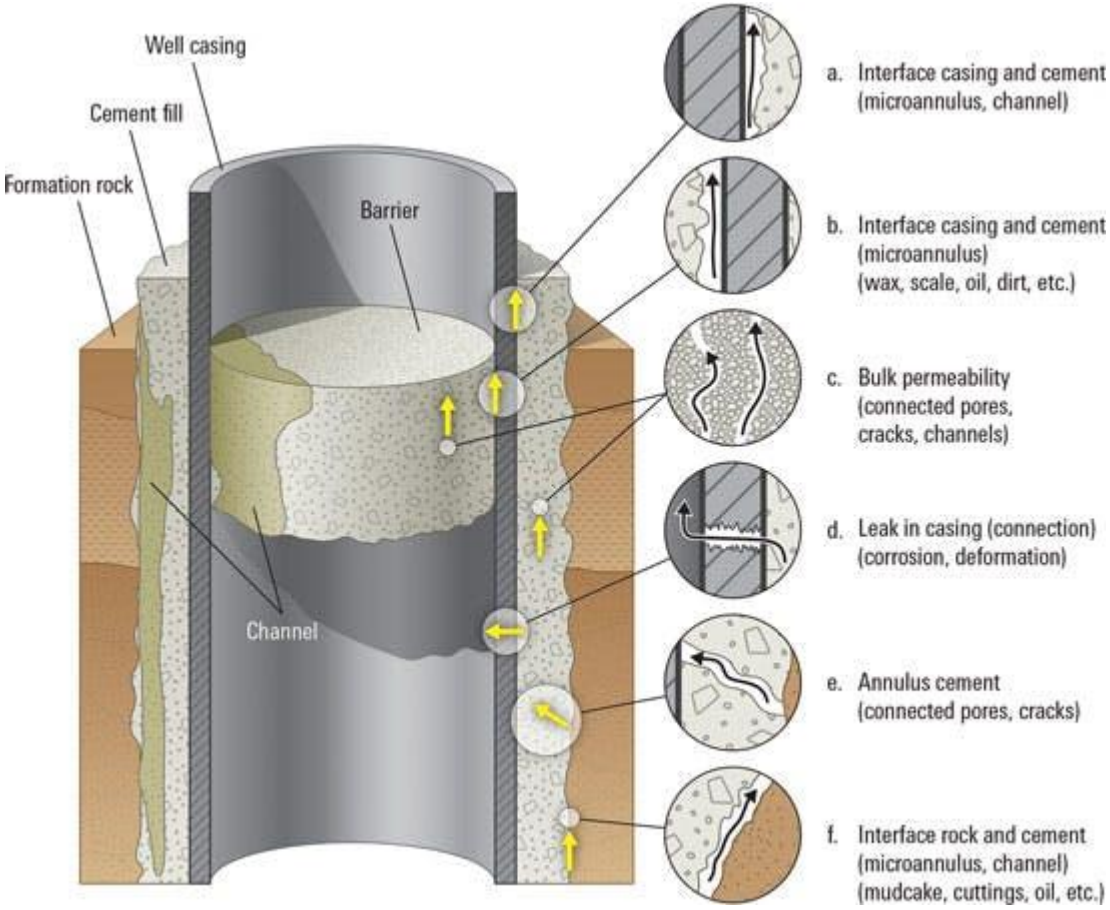

Figure 1. 3 Potential leakage pathways present in compromised cement [4]

To ensure long-term structural integrity, NORSOK D-010 defines well integrity as "the application of technical, operational, and organizational solutions to reduce the risk level of undesired formation fluid leaks throughout the life cycle of a well". [5]

NORSOK D-010 defined the requirement for cement properties to have an effective well barrier performance, such as the cement needs to:

a) Be impermeable.
b) Have long-term integrity.
c) Be non-shrinkable.
d) Be ductile (non-brittle), able to withstand mechanical loads/impact.
e) Have resistance to different chemicals/substances (H_2S, CO_2, and hydrocarbons)
f) Have Wetting, to ensure bonding to steel.

These criteria are set to ensure the right quality and allow long-term well integrity. However, well integrity surveys have shown that several wells have exhibited integrity issues. The petroleum safety authority (PSA) of Norway has conducted a survey on 71 wells, including 31 production and 40 injection wells, and found that cement accounted for 11% of failures. The results of all failures are shown in Figure 1. 4 below. [6]

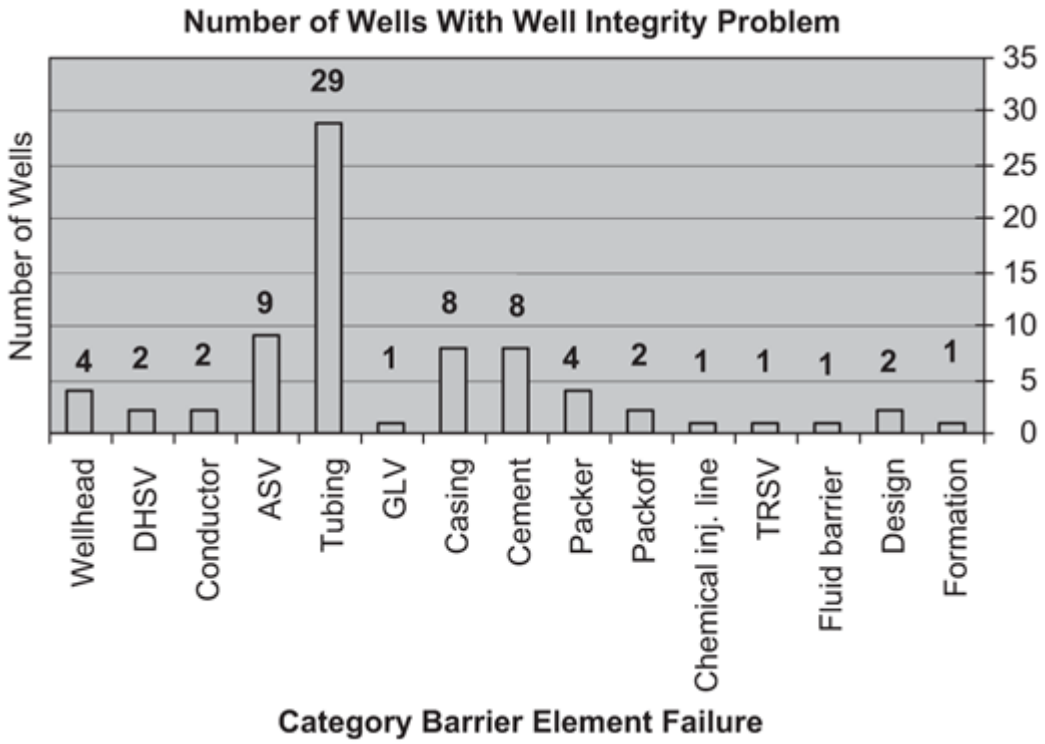

Figure 1. 4 Well integrity issues and WBE on NCS [6]

As seen in the integrity survey, this shows that the current cement does not satisfy the NORSOK D-010 standards and is prone to failure. This indicates improvements should be made to these well barriers. Improving current standard cement are already constantly in development. Moreover, geopolymer cement has also shown promising results in previous work, which will be reviewed in more detail in section 2.2 and with more research may be able to be an alternative to the current standard cement used.

The environmental side can also benefit from going from Ordinary Portland cement to geopolymer. In the making of 1-ton Ordinary Portland cement, it produces ~0,9-ton CO_2. While the making of 1-ton geopolymer produces ~0,3-ton CO_2 which indicates a reduction of ~67%. [28]

1.2 Problem Formulation

The current cement slurry formulas have shown to be sub-optimal for their applications. Currently, the industry is searching for alternative materials for plug and abandonment operations. Among others, geopolymer is one of the candidates and it is under research and development for its application in the oil well. Moreover, in recent years the application of nanoparticles has been studied and shown promising results in improving the performance of drilling fluid and standard cement. The application of nanotechnology may come to be one of the most efficient and cost-effective solutions to solve some of the current engineering problems faced today. Studies and research on the effect of nanoparticles on geopolymer are more limited, but early studies show promising results. Therefore, this thesis addresses the impact of **rock powder** and **nanoparticles** on the newly formulated geopolymer.

1.3 Scope and Objectives

The primary objective of this thesis is to investigate the issues addressed under the section problem formulation. This will be investigated through experimental and modeling works.

1.4 Research Methods

Figure 1. 5 outlines an overview of the structure of the research works performed in this thesis. The main activities include:

- Literature review on geopolymer research and impact of nanoparticles
- Examine the effects of Rock-powder and Nano-SiO_2 on the mechanical, petrophysical, and viscosity properties of geopolymer.
- Finally, develop an empirical model based on the destructive and non-destructive data of geopolymer.

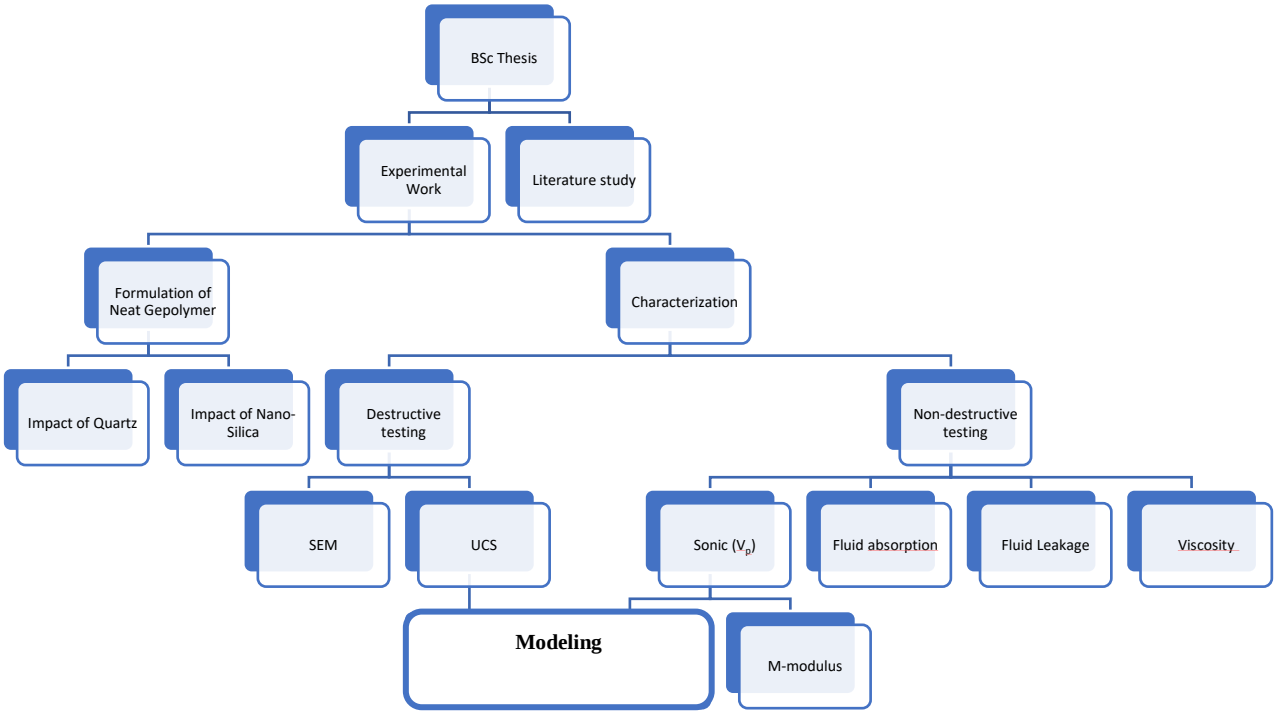

Figure 1. 5 Research Overview

2 Literature Study

The following section presents literature studies on alternative geopolymer formulations and the effects of various nanoparticles. As well as studies on conventional Portland cement. The previous research gave an insight into what chemicals, ratios, concentration, and curing time and temperature would be the better options to formulate the geopolymer with and without additives.

2.1 Ordinary Portland Cement (OPC)

Portland cement is a widely used binding material in the oil and gas industry due to its strength, availability, and economic feasibility. It is primarily used for well construction and P&A, and its slurry can be easily pumped and hardened rapidly [7]. The basic composition of Portland cement is a mixture of cement powder and water that undergoes a chemical process called hydration, resulting in the formation of a gelatinous phase called calcium silicate hydrate (CSH) [8]. However, it is essential to note that the conditions that Portland cement encounters in a well differ significantly from those encountered during construction operations. As a result, special Portland cement, such as class G and H, are designed with additives to meet the demands of specific well environments and operations.

The mineralogical composition of Portland cement clinker determines its properties, such as compressive strength and setting time. Portland cement clinker primarily consists of hydraulic calcium silicates, calcium aluminates, and calcium aluminoferrites, as well as one or more forms of calcium sulfate that are interground with the clinker [9]. To prepare a mixture that will produce Portland cement clinker, calcareous materials containing lime and argillaceous materials containing alumina, silica, and iron oxide are required. During the manufacturing process, frequent chemical analyses of all materials are made to ensure uniformity and high quality. The main oxides in conventional Portland cement clinker are CaO, SiO_2, Al_2O_3, and Fe_2O_3, which make up about 95% of its mineralogical composition [9].

One of the critical properties of Portland cement is its strength. After 8 hours of curing at 60°C, class G Portland cement mixed with a 0.44 water/solids weight ratio should have a compressive strength greater than 10.3 MPa according to the API standard [10]. However, at higher temperatures, a phenomenon called strength retrogression may occur, which can reduce the compressive strength of Portland cement within one month. To combat this issue, additives such as accelerators or retarders are used to modify the cement's basic composition. Other additives, such as weighting agents or extenders, can adjust the cement's hydrostatic pressure, density, or yield, while dispersants can disperse particles or fluids.

The API (American Petroleum Institute) classes of OPC are shown in Table 2. 1. The most common and frequently used classes within oil and wells are class G and H. In addition, it is common to design cement with additives to cover the different ranges of well depth and temperatures.

Table 2. 1 Portland cement classes for oil well cementing [11]

Class	Depth (ft)	Temperature F	Purpose
A	0–6000	80–170	Used when no special needs are required
B	0–6000	80–170	Used for conditions requiring moderate to high sulfate resistance
C	0–6000	80–170	Used for conditions requiring high early strength
D	6000–10,000	170–290	Used where high temperatures and pressure are found
G	0–8000	-	Used with accelerators and retarders to cover all range of well depth and temperatures
H	0–8000	-	Used with accelerators and retarders to cover all range of well depth and temperatures

As a reference, according to the API standard, the class G cement should be mixed with a 0,44 water/solid weight ratio. Meaning water content by weight divided by solid content by weight is equal to 0,44. After curing at 60°C for 8 hours, the API standard requires the cement to have a compressive strength greater than 10,3 MPa [10].

2.2 Previous works on Geopolymer

Table 2. 2 summarizes the application of nanoparticles on geopolymers, the characterization methods along with the key finding on the properties of the geopolymers. As shown in the table, nanoparticles have a positive impact on mechanical, elastic, rheological, and petrophysical properties. The performance of the nanoparticles varies from type to type, and the impact also depends on the concentration. From the literature study, we can observe that the right concentration of different nanoparticles can improve performance on geopolymer cement. The most promising results come from the addition of nano-SiO_2. One of the reasons is that the main ingredient in the geopolymer solid phase (Fly ash) is silica. Therefore, in this thesis, silica nanoparticles and quartz rock powder will be used for further investigation. The main reason for the selection of quartz is that it contains a large concentration of silica.

Table 2. 2 Review of the effect of nanoparticles

Author/ Reference	Nanoparticles and Characterization	Key findings
M.I. Abdul Aleem and P.D. Arumairaj (2012) [12]	Nanoparticle • None Test: • Compressive strength, 7 days, and 28 days	Results: • The results show that the optimum mix was Fly ash: Fine aggregate: Coarse aggregate with portions as follows; 1:1,5:3,3. • An alkaline solution of NaOH and $Na2SiO_3$ as an activator. The ratio of solution to fly ash was 0,35.

Sudipta Naskar and Arun Kumar Chakraborty (2016) [13]	Nanoparticle • Colloidal nano-silica (nS); 0,75% - 3% - 6% • Carbon nanotube (CNT): 0,02% • Titanium dioxide(TiO_2): 1% Test • Compressive strength • durability property test based on pH • Ultrasonic Pulse Velocity (UPV) • Rebound hammer	Results: • With the use of **1% TiO_2**, the compressive strength increases **32,96% increase for 7 days** **46,65% increase for 28 days** • The other nanoparticles reduced compressive strength in this study • pH remains almost constant (all) • UPV showed values greater than 4,5km/s, which proves the good quality of concrete for all cases. The TiO_2 values were very similar to the reference. • Rebound hammer predicted compressive strength did almost match for 7 days, but not for 28 days.
Han et al. (2022) [14]	Nanoparticle • Nano-Silica Characteristics • Compressive strength • Tensile strength • Microstructure • Hardening • Shear bond strength • Durability	Results: • Compressive strength got an increasing trend but then will decline if more is added. For 3wt% nano silica had a **42% increase after 3 days**. **18% after 27 days**. **14% after 56 days**. • Reduces the maximum tensile strength, but it is still recommended as the production of residual stress can reduce face destruction. Tensile strength reduced from ~1,36MPa (control) to 0,85MPa (NS2) – 0,8MPa (NS3) – 0,75MPa (NS4) • Gets more compact, with fewer unreacted particles. Resulting in higher strength, higher density, and lower porosity. Too much Nano-SiO_2 leads to a non-dense structure. • Accelerate the geopolymerization process (reducing setting time) High-calcium fly ash base: ~88min High-calcium fly ash with 3% silica: ~37min Low-calcium fly ash base: ~373min Low-calcium fly ash with 1,5% silica: ~255min • Improve the shear bond strength and bonding performance Adding 1wt% silica increased **Shear strength** by **~100% after 7 days, ~90% after 28 days, ~140% after 90 days** • Effectively improved the durability. Porosity reduced approximately by 10% for 2wt% of nano-silica The mass change was 2,01% for 2wt% silica compared to -3,95% for reference.

Assaedi et al. (2020) [15]	Nanoparticle • Nano-$CaCO_3$ Characteristics • Compressive strength • Flexural strength • Impact Strength • Hardness • Microstructure	Results: • Optimum amount, 1-2 wt% • Compressive and Flexural strength max increase was with 2wt% $CaCO_3$, Compressive strength went from 16,07 to 25,25 MPa. **(57% increase**) Flexural strength went from 2,71 to 4,30 MPa (**59% increase**) • Impact strength was best with 1wt% $CaCO_3$, from 6,73 to 10,11 kJ/m^2 (50% increase) • The hardness had the best results with 2wt% $CaCO_3$, from 86,7 to 93,8 HRH (8% increase) • Better bonding and cohesion between binder and different particles • The surface got rougher and more dense
Alvi et al. (2020) [16]	Nanoparticles • Al_2O_3 • MWCNT-OH Characteristics • Compressive strength • Shear Stress • Consistency • Static Fluid Loss • Indirect Tensile Strength • Sonic Strength • X-Ray • Microstructure and Elemental analysis	Results (both): • • Compressive strength increased (28 days), about **50% increase for MWCNT-OH** and about **43% for AL-0450** • Shear stress strength **increased by ~35%** • Stress-strain curves showed better load-carrying capacity and deformation, but mixtures became less ductile after 28 days. • Enhanced pumping time from ~1,5h to ~3h for both nanoparticles. (**100% increase)** • Viscosity increased (0,17-0,21-0,17 Pa to 0,19-0,27-0,23) • Little impact on Young's modulus. • MWNCT-OH increased tensile strength from 120 to 240 psi after 7 days (**100% increase)** and from 130 to 190 psi after 28 days (**46% increase)** • AL-0450 increased tensile strength by **~50%** after 7 days **and ~7%** after 28 days. • The UCS results show that the maximum strength develops in the early stages of curing. • Maximum sonic strength develops on the first day. • Geopolymer got denser and more compact (SEM). • In general, the mechanical strength improves and flexibility for a curing time of 7 days, but impact reduces for longer curing times. Results MWCNT: • Decreased fluid loss **(~45% decrease)** • Tensile strength improved after 7 days and 28 days Results AL-0450:

		• Increased fluid loss **(~16% increase)** • Tensile strength improved after 7 days, but little difference after 28 days
Duan et al. (2016) [17]	Nanoparticles • Nano-TiO_2 Characteristics • Compressive strength • Drying shrinkage • Carbonation • Microstructure	• Compressive strength got most significantly increased with 5% TiO_2. **The increase was 51% - 17,4% - 17,8% - 22,0% - 22,0% - 19,2% after 1 d, 3 d, 7 d, 28 d, 56 d, and 90 d, respectively**. • Drying shrinkage was most significantly improved with 5% TiO_2. After 28 days the reference had a shrinkage of ~1040 μm/m, while with the addition of 5% TiO_2, it was ~520 μm/m. **(Decrease of 50%).** • Carbonation depth is reduced with the addition of TiO_2, and most significantly with 5% TiO_2, with an approximate reduction **of 65%.** • Nano-TiO_2 will provide a result of a denser microstructure with fewer cracks.
Rahmawati et al. (2021) [18]	Nanoparticles • Nanos-Silica Characteristics • Direct tensile strength • Ductility • Compressive strength • Flexural strength • Fracture toughness • SEM analysis	The most effective amount of nano-silica was 2wt% for all tests. • Direct Tensile Strength reduced by 31% • Ductility improved by 152% • Compressive strength increased by 22% • Flexural strength increased by 82% • Fracture toughness increased • SEM images showed good nano-silica dispersion with fewer pores, and the matrix seemed denser.
Deb et al. (2015) [19]	Blends: 1. Fly ash only (Class F) 2. OPC blended fly ash 3. GGBFS blended fly ash Nanoparticles • Nano-Silica Characteristics • Workability • Setting time • Compressive Strength • SEM	The most effective amount of nano-silica was 2% for all blends and all tests. • All the geopolymer mixtures were flowing easily after mixing • The use of nano-silica reduces the setting time for all mixes. The mix with GGBFS reduced the time further, and with the OPC blend the setting time was the shortest • Compressive strength increased with the use of nano-silica. After 28 days, with 2% nano-silica, the compressive strength increased by; 129% (FA only), 128% (OPC mix), 88% (GGBFS mix) • The microstructure got denser and fewer unreacted particles

Zidi et al. (2021) [20]	Nanoparticles • Nano-Silica (5%) Characteristics • SEM images • Water absorption and density • Compressive strength • UPV • Setting time	• Improved homogeneity, matrix more compact, denser structure. • Density increased by 6% • Water absorption decreased by 10,5% • Compressive strength increased the most after 28 days with curing at 20°C, increasing 57%. • UPV increased from 3,16 to 3,82 Km/s • Setting time reduced from 360min to 45min
Phoo-ngernkham et al. (2014) [21]	Nanoparticles: • Nano-Silica • Nano-Al_2O_3 Characteristics: • SEM • Setting time • Compressive strength and E-modulus • Flexural strength • Shear bond strength	• Denser matrix and fewer non-reacted particles. The addition of more than 2% proved to be excessive. • Nano-SiO_2 significantly reduced setting time. Nano-Al_2O_3 had little effect on these contents. • Increased compressive strength - 2% nano-SiO_2, 31% (90d) - 1% nano-Al_2O_3, 43% (90d) • E-modulus increased • Flexural strength increased - 1% nano-SiO_2, 55% (90d) - 2% nano-Al_2O_3, 43% (90d) • Shear bond strength increased - 1% nano-SiO_2, 118% (28d) - 2% nano-Al_2O_3, 92% (28d)

3 Experimental works

This chapter presents the materials used, the geopolymer slurry preparation, the different characterization methods, and the theoretical description of the parameters obtained.

3.1 Materials

3.1.1 Water

The water used to make the cement slurries was fresh water from the laboratory's faucet. The water was assumed to be pure and free of contamination. Moreover, the water used most often for cement slurries in oil and gas fields is fresh water, so using a localized source of freshwater is realistic. A sample of water is shown in Figure 3. 1.

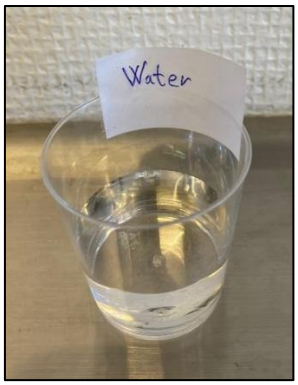

Figure 3. 1 Sample of freshwater

3.1.2 Ordinary Portland Class G Cement

The geopolymer slurries were compared with Portland class G cement. The cement was obtained from Heidelberg Materials (recently changed name from NORCEM AS). Table 3. 1 and Table 3. 2 show the composition of the cement. Portland class G is the most commonly used cement for oil well and is tested according to API SPEC 10A/NS-EN ISO 10426-1 [22].

Table 3. 1 Physical properties of Portland cement [22]

Density (lb/gal)	Surface Area (m^2/kg)	Max. Consistency (Bc)	Thickening time (Min)
16	317	13	108

*Table 3. 2 Chemical composition of Portland cement (*I.R =insoluble residue) [22]*

Cr(VI)	SO_3	C_3A	C_2S	C_4AF+2C_3A	Na_3O	MgO	IR*	Loss on Ignition
0,00%	1,73%	1,7%	55,6%	15,2%	0,48%	1,43%	0,1%	0,79%

The cement was mixed with a water/solid ratio of 0,44 as per API standards. Figure 3. 2 shows a sample of the cement powder.

Figure 3. 2 Sample of Ordinary Portland Cement

3.1.3 Geopolymer Components

Geopolymer gel is formed by a reaction between an alkaline activator and a solid binder. This section describes the components used.

3.1.3.1 Fly Ash

For this study, low-calcium fly ash class F was used, as seen in Figure 3. 3. The typical composition of fly ash is represented in Table 3. 3. The fly ash used was provided by Heidelberg Materials [22]. As shown in the table, SiO_2 and Al_2O_3 are the major components of fly ash.

Table 3. 3 Typical fly ash composition (%) [22]

SiO_2	Al_2O_3	Fe_2O_2	CaO	MgO	SO_3	Na_2O & K_2O
54,90	25,80	6,90	8,70	1,80	0,60	0,60

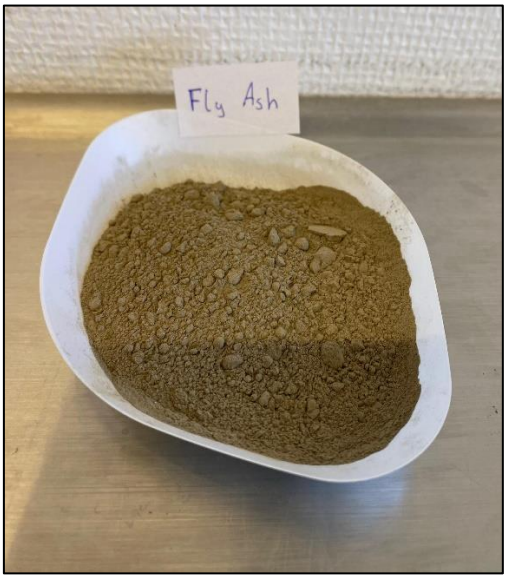

Figure 3. 3 Sample of Fly Ash

3.1.3.2 Alkaline Activator Liquid

For the geopolymer to go through the geo-polymerization, to form the binding gel, it is necessary for an alkali activator. The alkaline activator was created with a combination of Na_2SiO_3 and NaOH with a ratio of 2,5, which was based on the research from Hardjito et al. (2004) [29]. The alkaline liquid-to-solids ratio was 0,52, which is chosen based on the study performed by Adam et al. (2019) who showed the optimum compressive strength values. [30].

3.1.3.2.1 Na_2SiO_3

For this study, the sodium silicate (Na_2SiO_3) used was obtained from Merck Life Science AS/Sigma Aldrich Norway AS [37]. Figure 3. 4 shows a sample of the sodium silicate as well as the container. The solution has 45-65% of water content and a molar ratio of 1,6-2,6.

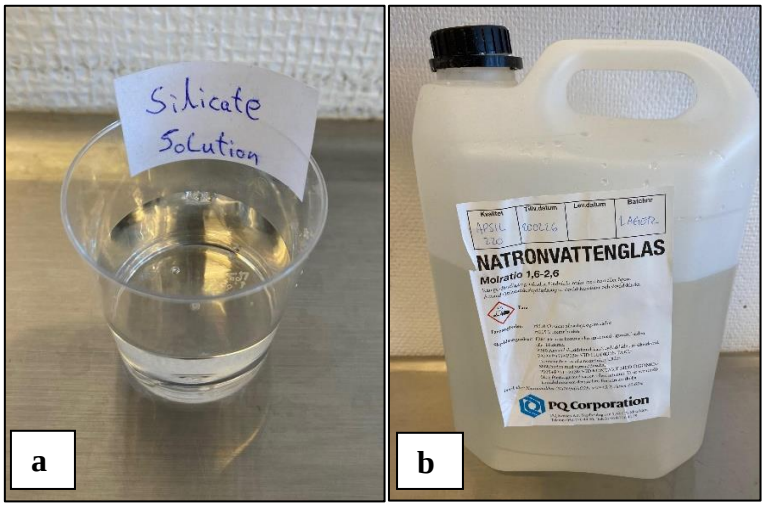

Figure 3. 4: a) Silicate solution. b) Silicate container

3.1.3.2.2 NaOH

The NaOH (Sodium Hydroxide) was obtained from VWR Chemicals of VWR International s.r.o. from the Czech Republic [23]. Figure 3. 5 shows the container, the NaOH pellets, and the 10M NaOH solution.

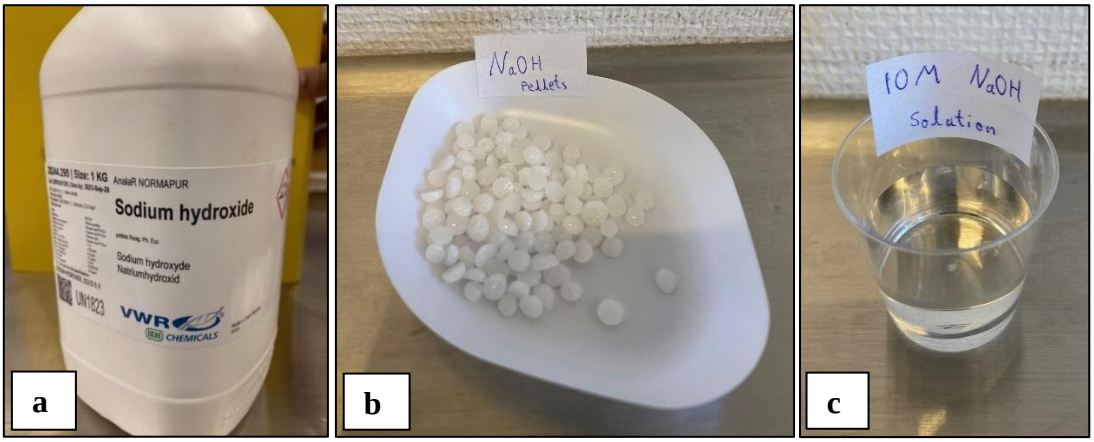

Figure 3. 5: Sodium Hydroxide a) container, b) pellets, c) solution

3.1.4 Description of Nanoparticles and Rock Powder

In addition to the base geopolymer, the additives used are presented in this section.

3.1.4.1 Rock Powder (Quartz)

The rock powder (Quartz) was obtained from North Cape Minerals Norway. The powder was crushed and strained out to obtain a size of less than 90µm. The average particle size before straining was mainly in ranges of 250 to 500µm. Figure 3. 6 shows quartz powder at < 90µm.

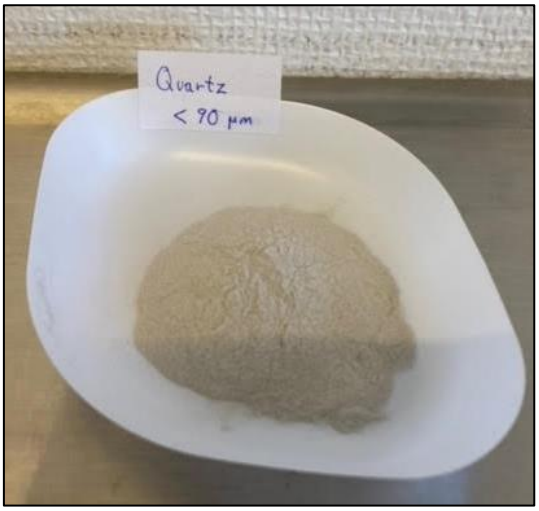

Figure 3. 6 Quartz powder, particle size < 90µm

3.1.4.2 Nano-SiO_2

The nano-silica is manufactured by Nyacol Nano Technologies, Inc. It is a colloidal mixture with a concentration of 50 wt.% suspended in H_2O. The density of the mixture is 1,4 g/mL at 25 °C and got a pH ranging from 9,0 – 10,5. Figure 3. 7 shows the SiO_2 solution. [34]

Figure 3. 7 SiO_2 solution

3.2 Sample Preparation

The following section describes the methods used to prepare and mix the chemicals to make the geopolymer samples.

3.2.1 Alkaline Solution

As described in section 3.1.3.2, the alkaline activator is composed of two components, the 10M sodium hydroxide solution and sodium silicate liquid.

3.2.1.1 10M NaOH Solution (Sodium Hydroxide)

The preparation of 10M NaOH is simple and consists of mixing the NaOH pellets with deionized water. Since the reaction is exothermic, the mixing was done gradually to avoid the solution getting too hot. When the solution was made, it was set in the cabinet for 24h before use to let the solution settle properly.

3.2.1.2 Sodium Silicate

The sodium silicate was bought and ready to use, no extra preparation was needed.

3.2.2 Slurry and Geo-polymerization

Firstly, all the chemicals and components are weighed up, then the next step is to mix the sodium silicate with the 10M sodium hydroxide. The mix was stirred by hand for 10 seconds, before being poured over to the solids. This was then hand-stirred for 2-4 minutes. To improve workability, extra water is now added. The slurry is then poured into plastic molding cups. The cups with the slurries are left at rest for 1 day before being put in the oven. This is because the curing happens in ambient pressure, so to avoid the binder evaporating the geopolymer rests for 1 day. The oven maintains a temperature of 62 °C and ambient pressure for 4, 7, and 10 days. After the cups have been in the oven, they were left to rest for 1 day at room temperature before testing.

To get better representative results, there were generally made 3 plugs for each batch of slurry, representing the exact mixture. The dimension of the plastic cups used are 68,2mm in height, and 32,8mm in inner diameter, depictured below in Figure 3. 8.

Figure 3. 8 Plastic cups used for molding.

3.2.3 Cutting and Polishing after Curing

To get a representative sample that will provide consistent results when testing, it was needed to remove the top layer of the plugs due to free water and expansion. This top layer contains fewer solids and more fractures and pores. To remove this and get a smooth horizontal top surface, cutting and/or polishing were performed depending on the condition of the plugs.

3.2.3.1 Cutting

The machine Struers Discotom-5 was used to remove the top part of the geopolymer plugs. Figure 3. 9 shows a picture of the machine and setup.

Figure 3. 9 Different angles of the Struers Discotom-5

3.2.3.2 Polishing

For the final touch, the plugs were polished with sandpaper to make the top surface uniform and horizontal. Without a uniform surface, the uneven or inclined part can generate huge stress, resulting in poor results. A water lever was used to reduce the uncertainty of point load effects by verifying the horizontal top surface. The sandpaper used was purchased from Clas Ohlson and had a grain size of 120 and the brand was Bosch, see Figure 3. 10.

Figure 3. 10 Bosch sandpaper

3.3 Characterization Methods

Figure 3. 11 Scope of experimental testing Figure 3. 11 shows the scope of characterization methods to be used. There are two categories of testing. Non-destructive testing, which includes characterization with ultrasonic, mass absorption, and rheology. The other is destructive testing, which includes a uniaxial compressive test, and then remains to be tested with SEM analysis.

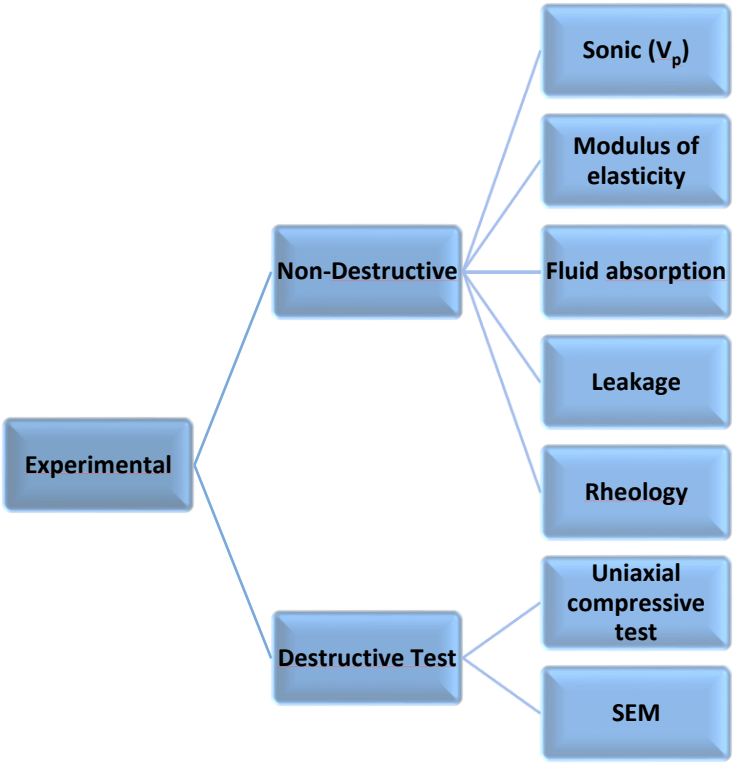

Figure 3. 11 Scope of experimental testing

3.3.1 Sonic Travel Time

Ultrasonic inspection is a non-destructive technique for evaluating a material's capability to transmit mechanical sound waves throughout its body. The travel time will vary depending on the strength of the specimens due to the content of cracks, pores, trapped air, or bad mixing. In general, the travel time will be lower for materials that are strong and well-compacted. Figure 3. 12 displays the setup used in ultrasonic testing, where ultrasonic pulses are sent through the specimens, and the travel time from the transmitter to the receiver on the opposite side of the material is recorded.

To calculate the compressional wave velocity the length of the specimen and the travel time are used as shown in Equation 3. 1.

Equation 3. 1

$$V_p = \frac{L}{t}$$

Where:

- $V_{p,}$ the P-wave's velocity (m/s)
- L, the length of a plug (m)
- t, the P-wave's travel time through the specimen (in seconds)

The photograph in Figure 3. 12 showcases the CNS Farnell Pundit 7 device used to measure the travel time through the specimens. Before testing, the measuring equipment is calibrated using a calibration plug with a travel time of 25 µs. The surface of the plugs at the top and bottom must be in close contact with the metallic surfaces of the source and receiver transducer.

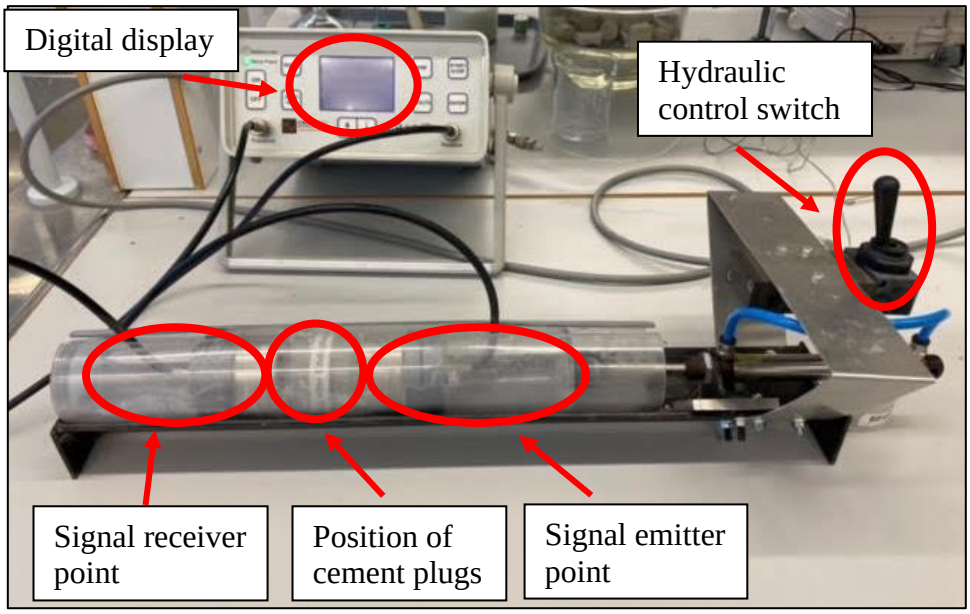

Figure 3. 12 CNS Farnell Pundit 7 device

3.3.2 Modulus of Elasticity (P-wave Modulus)

P-wave modulus is a measurement of the elasticity of a material. It describes the ability of a material to withstand compression. The P-wave modulus definition is the ratio of axial stress to axial strain in a uniaxial strain state. [24]

The relation between the P-wave modulus, the bulk modulus, and the shear modulus are as shown in Equation 3. 2:

Equation 3. 2

$$M = K + \frac{4G}{3}$$

The compressional wave velocity is related to the bulk modulus and the shear modulus with the following equation:

Equation 3. 3

$$V_p = \sqrt{\frac{K + \frac{4G}{3}}{\rho}}$$

This can be rewritten as:

Equation 3. 4

$$V_p^2 * \rho = K + \frac{4G}{3}$$

Substituting Equation 3. 4 into Equation 3. 2, and dividing by 10^9 to get GPa, gives:

Equation 3. 5

$$M = \frac{V_p^2 * \rho}{10^9}$$

- M, P-wave modulus (GPa)
- K, Bulk modulus (GPa)
- G, Shear modulus (GPa)
- ρ, Density of the given plug (kg/m^3)
- V_p, Compressional wave velocity (m/s)

V_p is calculated from the ultrasonic travel time, described in section 3.3.1 above.

The bulk modulus represents a material's ability to resist uniform compression by quantifying the volume change in response to applied pressure. A larger bulk modulus implies the material is less susceptible to compression.

The shear modulus, or the modulus of rigidity, characterizes a material's resistance to deformation under shear stress. It measures the alteration in shape when shear stress is applied. A greater shear modulus signifies a higher resistance to deformation due to shear forces.

3.3.3 Fluid Absorption

The porosity and permeability of the specimen's internal structures are used to determine the capacity for fluid to flow through it. To evaluate this, the internal structure was studied indirectly by studying mass absorption. If the specimen gets an increase in water absorption it is generally considered unfavorable as this indicates fluid may migrate through the geopolymer. Increased water absorption can also be an indication of a weak microstructure or cracks, which can result in poor integrity in the geopolymer at a later stage. To calculate the percentile mass change of the specimen after being immersed in water for 24h, Equation 3. 6 was used:

Equation 3. 6

$$\Delta M = \frac{M_t - M_0}{M_0} * 100$$

Where:

- ΔM, the change of mass (%)
- $M_{0,}$ mass before immersion in water
- $M_{t,}$ mass after a set time in water

3.3.4 Leakage

According to NORSOK D10, cement should have the property of non-shrinkage. The reason is that if cement shrinks, it creates a leak path between the casing and the cement. To evaluate the shrinkage properties, a simplified leakage test was performed on the geopolymer mixtures with and without nano-silica and compared with the OPC. The mixtures were poured into pipes and put in the oven for 10 days and 1 day at rest before testing. Then water was added on top of the

pipes and set to rest for 24h to later check if any water had leaked through. Figure 3. 13 shows the setup for the test.

Figure 3. 13 Test setup for leakage testing

3.3.5 Rheology

Rheology is the study of how materials flow, or deform, in response to external stress. The behavior will depend on various conditions, such as temperature, pressure, and applied stress. The knowledge of the rheological properties of the fluids used in the petroleum industry is highly important due to the amount of fluid transportation. Especially for drilling fluid and cement, this is because if the viscosity of the cement gets too high the pumps may not be able to pump or displace the cement properly.

Figure 3. 14 shows the Fann Viscometer, which was used to measure the viscosity of the geopolymer and cement slurries. The testing was conducted at atmospheric pressure and a standard temperature of 20 °C. The viscometer responses of the slurries were measured at 300, 200, 100, 60, 30, 6, and 3 revolutions per minute (RPM).
To describe the rheology of the slurries, there are several models available. However, in this thesis, the Casson model will be used since the model is commonly used to describe the rheology of cement. The Casson model is a two-parameter model, which describes fluids from low to high shear rates. It is a function of yield stress and plastic viscosity. [25]

Equation 3. 7

$$\tau^{0,5} = \tau_c^{0,5} + \mu_c^{0,5}\gamma^{0,5} \quad For\ \tau < \tau_c$$
$$\gamma = 0 \quad For\ \tau \geq \tau_c$$

Where:

- τ, measured shear stress (Pa)
- τ_c, yield stress (Pa)
- μ_c viscosity (Pa.s)
- γ shear rate (sec^{-1})

Figure 3. 14 Fann Viscometer

3.3.6 Compressive Strength (UCS)

The concept of Uniaxial Compressive Strength involves evaluating the ability of a material to withstand compression until it breaks. This is a well-established method in destructive testing to determine the compressive strength of a material. In addition, non-destructive methods can also be utilized to estimate the compressive strength.

To conduct the series of compressive strength tests, the Uniaxial compressive test apparatus was used, as shown in Figure 3. 15. The software program, catmanEASY, was connected to the apparatus and recorded the compressive data. The start position was set based on the height of the specimen, which was then placed and centered between two loading plates for crushing. The force was reset to zero before starting the test and the axial load was continuously applied to the specimen until it was crushed.

The data received from the tests is simply the force used on the specimen. To calculate the uniaxial compressive strength (UCS) we divide the force required to crush the specimen by the cross-sectional area of the specimen [26].

Equation 3. 8

$$UCS = \frac{F_{max}}{A}$$

Where:

- UCS, the Uniaxial compressive strength (MPa)
- F_{max}, the force used at the time of failure (N)
- A, the cross-sectional area of the specimen (mm^2)

Figure 3. 15 Photo of the Uniaxial compressive Test apparatus

3.3.7 Scan Electron Microscope (SEM)

Unlike the ordinary microscope that uses light, SEM uses electrons to form an image. Compared to a traditional microscope, the SEM got several advantages such as a larger depth of field, which allows it to focus on more of the specimen at the same time. It also got a higher resolution, making it possible to magnify the image at much higher levels. Since the SEM uses electrons instead of lenses, the user has way more control over the degree of magnification. [27]

After the uniaxial compressive strength test, a sample of the remains will be sent for a SEM examination. The use of SEM will give valuable insight into the characterization of the internal structure of the geopolymer and provide valuable information on the impact of the nanoparticles added. Figure 3. 16 shows the SEM equipment.

There are several types of images the SEM can take, but the two used in this thesis are; Secondary Electron 2 Images and Backscattered Electron Detector Images.

- Secondary Electrons are electrons with a lower energy level, and because of this, these electrons originate from the surface of the sample. This makes this type of image very useful for examination of the surface morphology (structure, formation, and classification). These images are also the ones that provide the highest resolution. [31]
- Backscattered electrons are electrons with higher energy that re-emitted from the sample due to elastic scattering by the atoms. These electrons are useful for revealing the chemical compositional differences, or atomic number contrast. This is important when doing element analysis. The resolution is however lower due to the larger source size of the electrons used. [31]

Figure 3. 16 Zeiss Gemini Supra 35 VP SEM Equipment

3.3.8 Empirical UCS vs Vp Model

In literature, several empirical models that relates Uniaxial compressive strength to the compressional wave velocity are available. The models are extracted based on the rock material, and cement. Therefore, their applicability and prediction are limited.
In chapter 5, geopolymer dataset based empirical model will be derived. The performance of this thesis's model predictions will be compared with rock-based empirical model (Horsrud, 2001) [35] and cement based empirical model (Titlestad, 2021)[36]. The models read:

Horsrud's model:

Equation 3. 9

$$UCS(MPa) = 0.77V_p^{2.93}$$

Where, Vp is compressional wave velocity (km/s)

Titlestad's model:

Equation 3. 10

$$UCS(MPa) = 0.2191 \cdot V_p^{3,9503}$$

Where, Vp is compressional wave velocity (km/s)

3.4 Experimental Testing and Test Designs

For this thesis, there were three phases, corresponding to the three test designs made. Consisting of phase 1: formulation of neat geopolymer, phase 2: studying the effect of replacing a portion of fly ash with quartz, and phase 3: studying the effect of adding nano-silica. The following

sections will describe the test designs and the idea behind them. In addition to the 3 different designs, a batch of ordinary Portland cement was made to be able to compare the results with the commonly used cement in the oil and gas industry today. The Portland cement was mixed with a water/solid ratio of 0,44 as per API standards.

A simplified overview of the testing done is shown in Figure 3. 17 below. Phase 1 is to formulate a neat geopolymer mixture that can be an alternative to OPC in oil well cementing operations. Continuing to phase 2 to investigate the effects of quartz, and then phase 3 to study the effect of nano-silica, on the newly made geopolymer mixture.

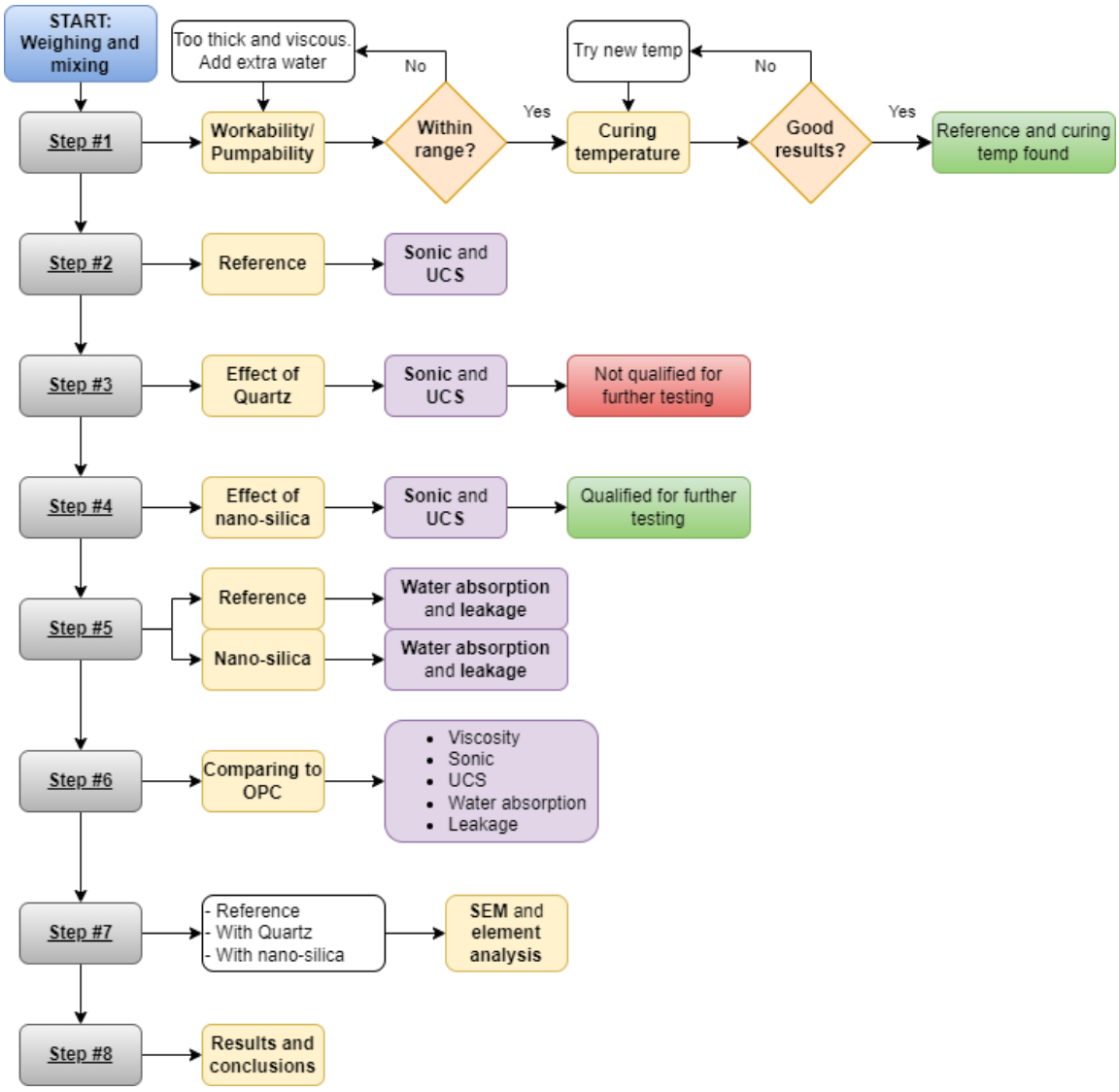

Figure 3. 17 Simplified overview of the testing

3.4.1 Test Design Phase 1: Formulation of Neat Geopolymer

Design idea: The idea is to formulate a neat geopolymer cement that can be an alternative to the ordinary Portland cement commonly used today in the oil and gas industry. The right composition of geopolymer could have improved capabilities compared to OPC. The first obstacles to geopolymer however, are its high viscosity, and finding a suitable curing

temperature. Therefore, the first task is to make sure the geopolymer mixture is pumpable and find a suitable curing temperature.

The starting mixture can be seen in Table 3. 4. The key takeaways are the Silicate/NaOH ratio of 2,5 and the Alkaline liquid/solids ratio of 0,52. These contents and ratios were held constant for all further test designs.

Table 3. 4 Content in starting mixture

Fly ash (g)	10M NaOH (g)	Silicate (g)	Silicate/NaOH ratio	Alkaline liquid/solids ratio
202	30	75	2,5	0,52

Screening process: Figure 3. 18 shows the screening process we start with to find a suitable neat geopolymer. Where the first criteria are workability, followed by curing temperature.

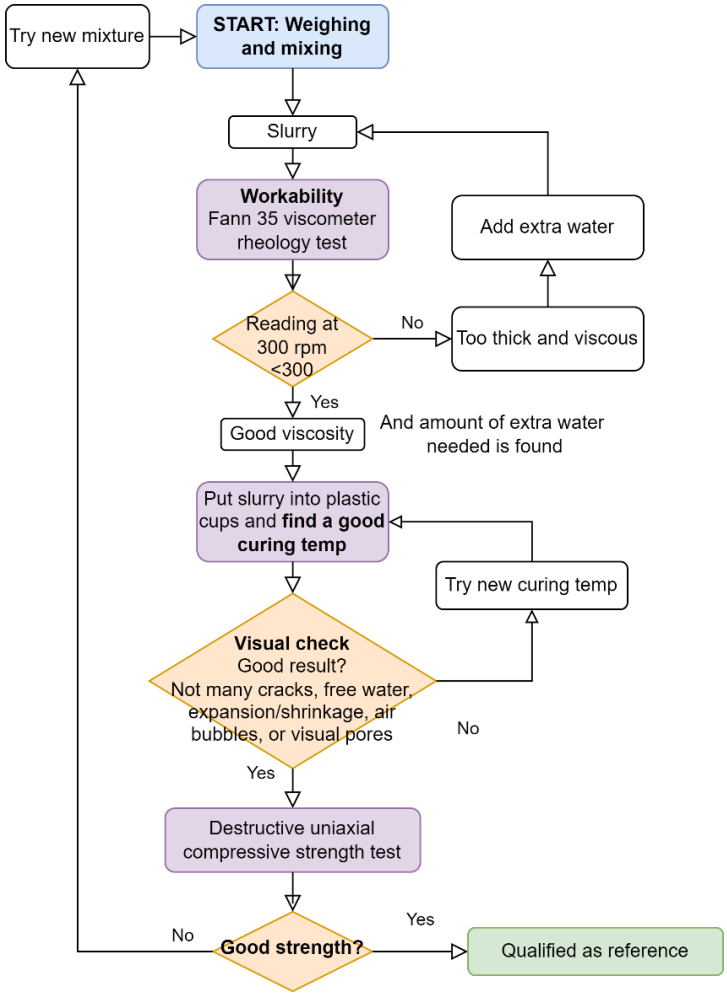

Figure 3. 18 Screening process

Workability/Pumpability: To improve pumpability, extra water was needed. The criteria for pumpability were viscosity within range, meaning 300rpm had a reading on the rheometer (θ300 > 300). Therefore, extra water was added in small steps and tested until this was reached. A total of four geopolymer mixtures with varying content of extra water was made, shown in Table 3. 5 Content of extra water and corresponding new liquid/solid ratios. The names correspond to the content of water, e.g., "W10" refers to 10g of water added.

Table 3. 5 Content of extra water and corresponding new liquid/solid ratios

Name:	W0	W10	W15	W20
Fly ash (g)	202	202	202	202
10M NaOH (g)	30	30	30	30
Silicate	75	75	75	75
Extra water	**0**	**10**	**15**	**20**
Silicate/NaOH ratio	2,5	2,5	2,5	2,5
Alkaline liquid/solids ratio	0,52	0,52	0,52	0,52
Total liquid/solids ratio	0,52	0,57	0,59	0,62

Curing: For curing a temperature of 62°C and 105°C were tested. The reason for choosing a temperature of 62°C was due to previous research where a temperature of 60°C to 65°C was quite successful [32] [33]. The mixture used was "**W20**".

3.4.2 Test Design Phase 2: Formulation of Geopolymer Replacing a Portion of Fly Ash with Quartz

Design idea: The main component of the geopolymer is fly-ash, and the main minerals in fly ash are silica (~55%) and aluminum (~26). Quartz also got high contents of silica, the hypothesis was therefore if quartz could create a good bond and improve the strength of the geopolymer mixture by replacing various content of fly ash with quartz. The quantity was replaced instead of just added on top so that the Alkaline liquid/solid ratio was kept at a constant of 0,52 as previously mentioned.

Test Design: Fly ash of quantities 10g, 20g, and 30g was replaced with quartz to look at the effect as shown in Table 3. 6. "Q10" represents 10g quartz in the mixture. The quartz used for all batches had a size of less than 90µm.

Table 3. 6 Test Design Phase 2, quartz content

Name:	Q10	Q20	Q30
Fly ash (g)	192	182	172
Quartz (g)	10	20	30
NaOH (g)	30	30	30
Silicate (g)	75	75	75
Water (g)	20	20	20
Alkaline l/s ratio	0,52	0,52	0,52
Total l/s ratio	0,62	0,62	0,62

3.4.3 Test Design Phase 3: Formulation of Geopolymer with the Addition of Nano-Silica

Design idea: Nanotechnology has shown promising results before as previously mentioned in section 2.2 . Following the same idea as test design 2, the addition of nano-silica will be tested due to the high content of silica in fly ash.

Test Design: Nano-silica in liquid form was added with varying content of 0,15g, 0,35g, and 0,55g. To keep the ratios the same, the mixtures had the same amount of water reduced, as shown in Table 3. 7. "S15" represents 0,15g content of nano-silica.

Table 3. 7 Test Design Phase 3, nano-silica content

Name:	S15	S35	S55
Nano-silica (g)	0,15	0,35	0,55
Water (g)	19,85	19,65	19,35
Fly ash (g)	202	202	202
NaOH (g)	30	30	30
Silicate (g)	75	75	75
Alkaline l/s ratio	0,52	0,52	0,52
Total l/s ratio	0,62	0,62	0,62

4 Results and Discussion

4.1 Phase 1 Results

4.1.1 Screening results

Due to the availability of the experimental setup, the geopolymer screening was based on viscosity and temperature. These were evaluated at atmospheric pressure.

4.1.1.1 Viscosity reading

During geopolymer synthesis, the first task was to investigate the slurry pumpability/workability**.** This was evaluated through a viscometer. Table 4. 1 shows the viscometer dial readings with varying content of extra water. The maximum limit for the viscometer is 300 dial readings. The θ300 RPM (θ300) greater than 300 means that the viscosity of the slurry is beyond the limit and hence, the slurry was added with extra water to make it thin. As seen in the table, after four attempts (for 0g, 10g, and 15g), the 20g of extra water blended geopolymer slurry could provide a reading at 300 RPM. Initially the mixing was done by hand, but the mixture with 20g extra water was also tested after mixing it in a mixer. Adding more water, the slurry would be thinner. however, more water will reduce the strength of the geopolymer. Therefore, in this thesis work, 20 g extra water was selected for the geopolymer synthesis.

A more in-depth rheology test will be presented later in section 4.4.3 Rheology.

Table 4. 1 Viscosity dial reading

Extra water:	300rpm	200rpm	100rpm	60rpm	30rpm	6rpm	3rpm
0g				**θ300 > 300**			
10g (hand mix)		**θ300 > 300**	187				
15g (hand mix)	**θ300 > 300**	260					
20g (hand mix)	**267**	176	88	54	27	6,5	3,5
20g (with mixer)	**248**	166	83	51	25	6,5	4

4.1.1.2 Curing Temperature

The temperature was also one of the screening factors used for the geopolymer synthesis.
Curing at 105°C: After one day in the oven at 105°C the plugs had significant expansion and got several cracks, illustrated in Figure 4. 1 below. These plugs were therefore taken out and a curing temperature of 105°C was disqualified.

Curing at 62°C: After 4 days in the oven, the plugs had no cracks and less expansion than for 105°C. Therefore, the curing temperature of 62°C was chosen to be used for further testing.

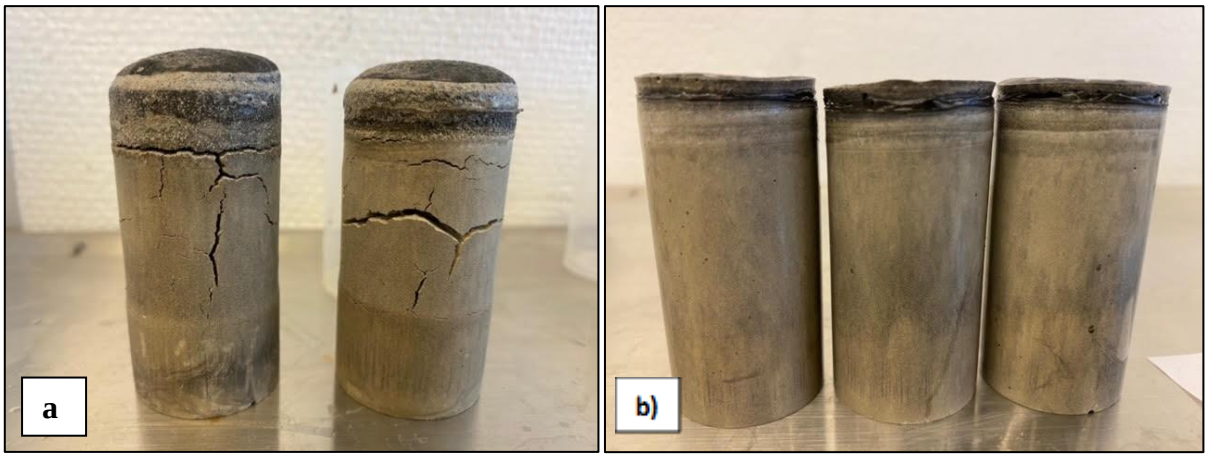

Figure 4. 1 a) Plugs after 1 day curing at 105°C, and b) plugs after 4 days curing at 62°C

4.1.2 UCS

The same 3 plugs from screening were cut and polished, as seen in Figure 4. 2, prepared for sonic and UCS testing. This was the starting point, but later the same mixture was also tested after 7 and 10 days of curing at 62°C. Figure 4. 3 depicts plugs after 10 days of curing and after polishing, and Figure 4. 4 depicts plugs after 7 days of curing and before polishing.

Figure 4. 2 Reference (GP) plugs out of the oven (4 days, 62°C) after polishing

Figure 4. 3 Reference (GP) plugs out of the oven (10 days, 62°C) after polishing

Figure 4. 4 Reference (GP) plugs out of the oven (7 days, 62°C) before polishing

For a better evaluation, the properties of the neat geopolymer were compared to Ordinary Portland Cement (OPC) which was tested after a curing time of 4 and 10 days. After being instructed by the supervisor, 0,44 water-cement ratio (WCR) of the G-class cement plug was prepared and tested with one of the 2023 MSc candidates, who is working on a different geopolymer research project. Figure 4. 5 illustrates the strength development after different curing times. The strength for geopolymer reference increases significantly from 4 to 7 days of curing and reduces from 7 to 10 days of curing. The increase in strength indicates that the geopolymer needs more than 4 days to crystalize and get strong bonds at a temperature of 62°C. The reduction from 7 to 10 days may indicate a temperature-degrading effect. Moreover, the strength of the geopolymer compared to OPC is higher, but the graph implies that geopolymer may need a longer time to achieve its highest strength, as the strength was close to equal after 4 days of curing.

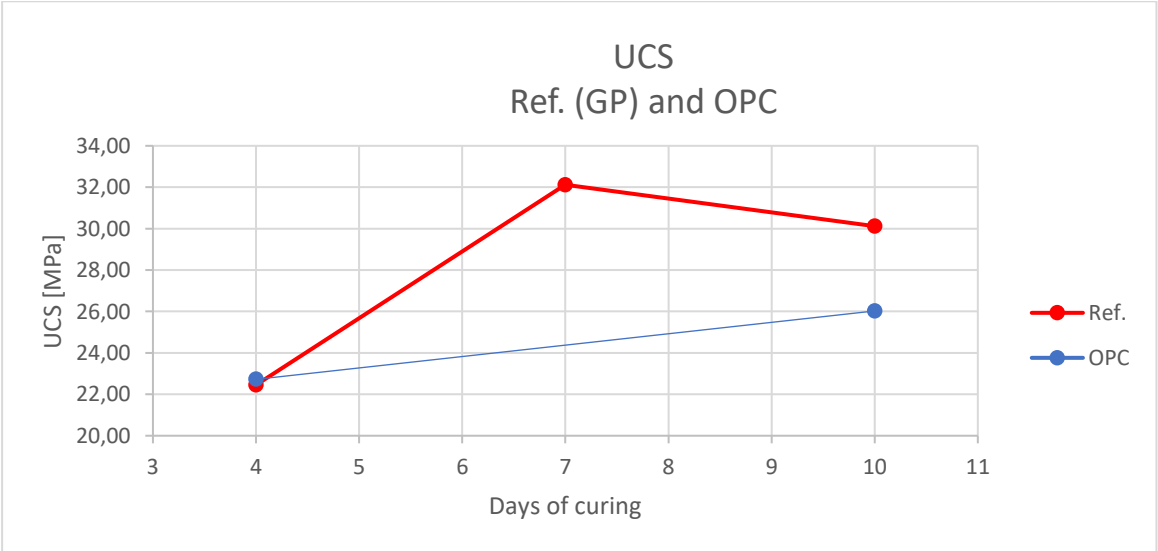

Figure 4. 5 Graphical representation of the UCS development of reference GP and OPC

Figure 4. 6 shows the UCS results after 4- and 10-days side by side respectively, where the red is geopolymer and the blue OPC. The left bars with a dark color represent 4 days, and the lighter color 10 days. The high standard deviations may be due to point load on some samples.

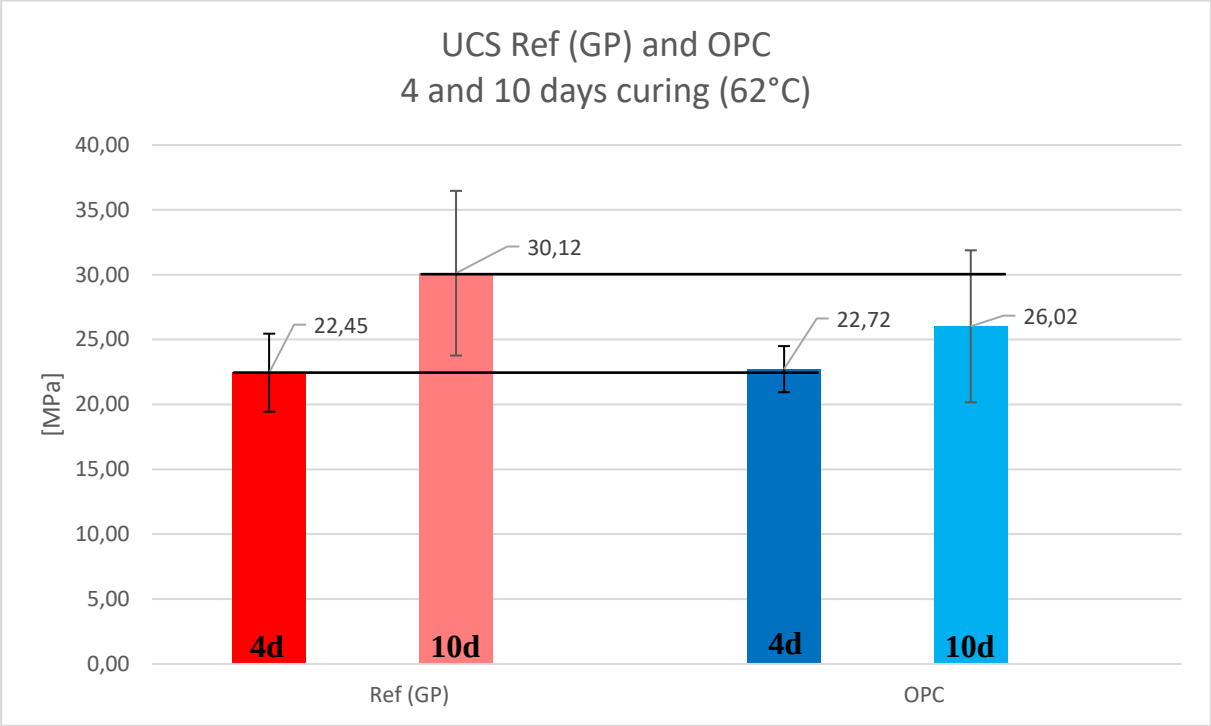

Figure 4. 6 UCS ref (GP) and OPC results after 4 and 10 days of curing, with standard deviations

4.1.3 Water Absorption and Leakage

Water absorption and Leakage tests will be presented in sections 4.4.1 and 4.4.2 under 4.4 Further characterizations, where it is compared to geopolymer with nano-silica and with OPC.

4.2 Phase 2 Results

4.2.1 UCS

Plugs with varying content of quartz were made to perform UCS tests after different time periods. For geopolymer with quartz UCS-testing was performed after 4 and 10 days of curing. Figure 4. 7 shows the first plugs with quartz after polishing ready for sonic and UCS testing.

Figure 4. 7 Plugs out of the oven (4 days, 62°C) after polishing. a) 10g Quartz. b) 20g Quartz. c) 30g Quartz

Below in Figure 4. 8, the UCS results for the quartz system are presented, as well as the geopolymer reference colored in red. The quartz system after 4 days had a slight increase with 10g quartz added compared to the reference, but a slight decrease with 20g and 30g quartz. However, the strength increased again after 10 days to slightly be higher than the geopolymer reference. This result could imply that the addition of quartz increases the time needed for geopolymerization during curing, curing time of 28 days would have told us more. However, due to the limited thesis duration, this was not performed, and it is recommended as future work.

Given the results we have, we cannot tell if the strength would have improved even more after a longer curing time. At the time with the results at hand, the conclusion was that quartz didn't significantly improve the strength enough to continue with further testing on the quartz system. Instead, phase 3 was initiated. However, in retrospect, the quartz system due to its high silica content seems more promising than first thought, and more testing should have been performed.

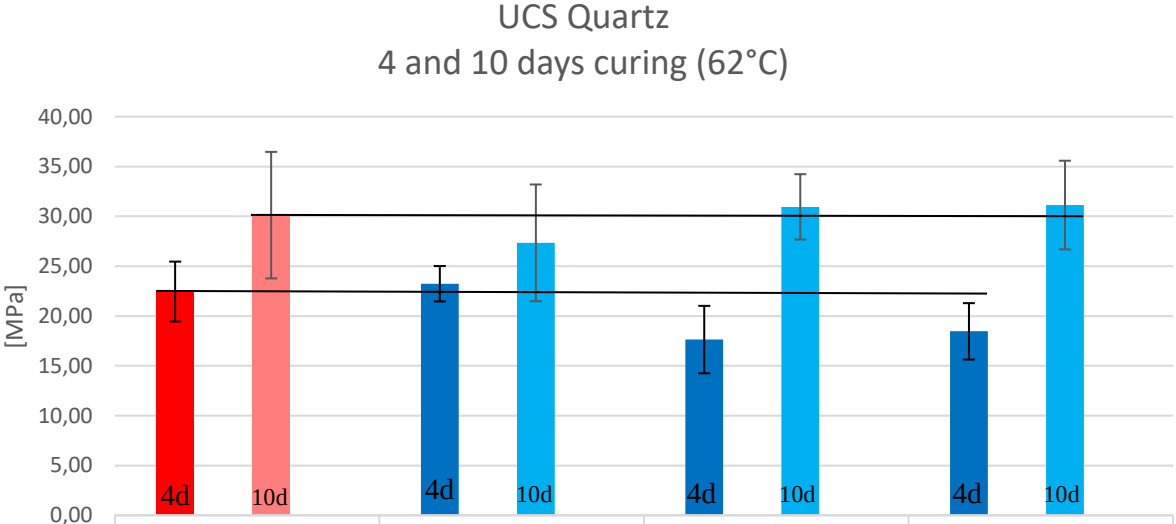

	Ref (GP)	GP+10g Quartz	GP+20g Quartz	GP+30g Quartz
4d UCS	22,45	23,24	17,63	18,46
4d std	3,01	1,78	3,38	2,83
10d UCS	30,12	27,34	30,95	31,13
10d std	6,35	5,86	3,28	4,45

Figure 4. 8 UCS Quartz results after 4 and 10 days of curing, with a standard deviation

4.2.2 Water Absorption and Leakage

Since results were at the time considered not good enough, phase 2 shifted to phase 3, and therefore water absorption and leakage tests were not conducted on phase 2, nor the more in-depth rheology test.

4.3 Phase 3 Results

4.3.1 UCS

Plugs with varying content of nano-silica were made to perform UCS tests after different time periods. For geopolymer with nano-silica UCS-testing was performed after 4 and 10 days of curing. There are 5 plugs for 10 days curing for 0,55g due to a little portion was spilled during mixing, so an extra batch for 0,55g nano-silica was made.

Figure 4. 9 and Figure 4. 10 show the plugs with nano-silica after 10 and 4 days of curing, respectively. Left to right increasing the amount of nano-silica, steps 0,15g, 0,35g, and 0,55g.

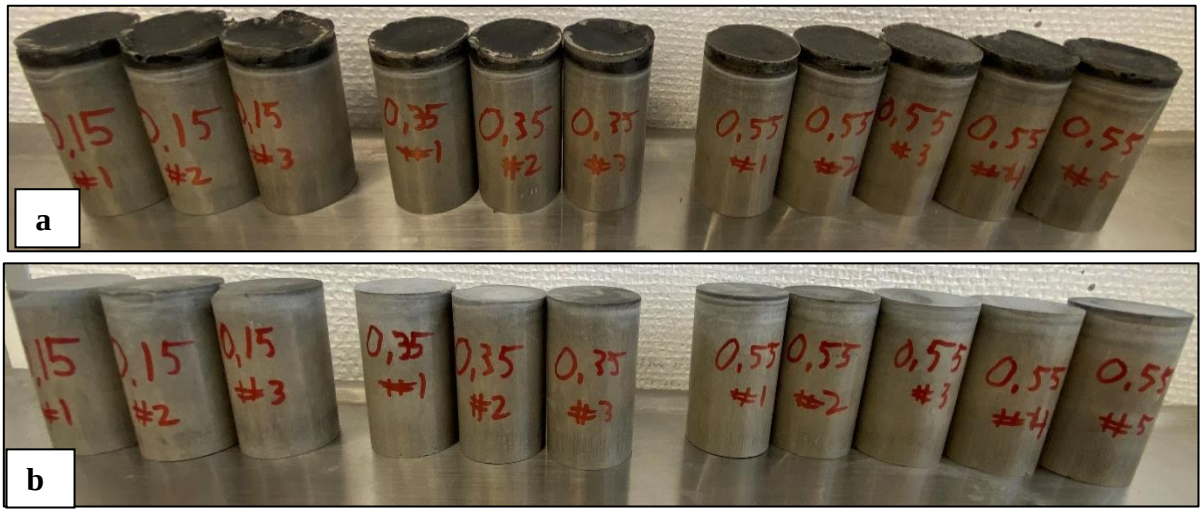

Figure 4. 9 Plugs out of the oven (10 days, 62°C). a) Before polishing. b) After polishing

Figure 4. 10 Plugs out of the oven (4 days, 62°C). a) Before polishing. b) After polishing

The UCS results are presented in Figure 4. 11 UCS Nano-Silica (NS) after 4 and 10 days of curing. The strength of the nano-silica system decreased for both 4 and 10 days of curing. However, for both 4 and 10 days of curing, the nano-silica system shows an increasing trend

with the increased amount of nano-silica added. This implies that the optimum amount of nano-silica added may not have been found, and with this optimum amount, the strength could have been improved beyond the strength of the reference. Another cause for the decrease of strength, as mentioned for phase 2, may be due to the addition of nano-silica increasing the geopolymerization time. A longer curing time may be needed for the nano-silica to improve the geopolymer.

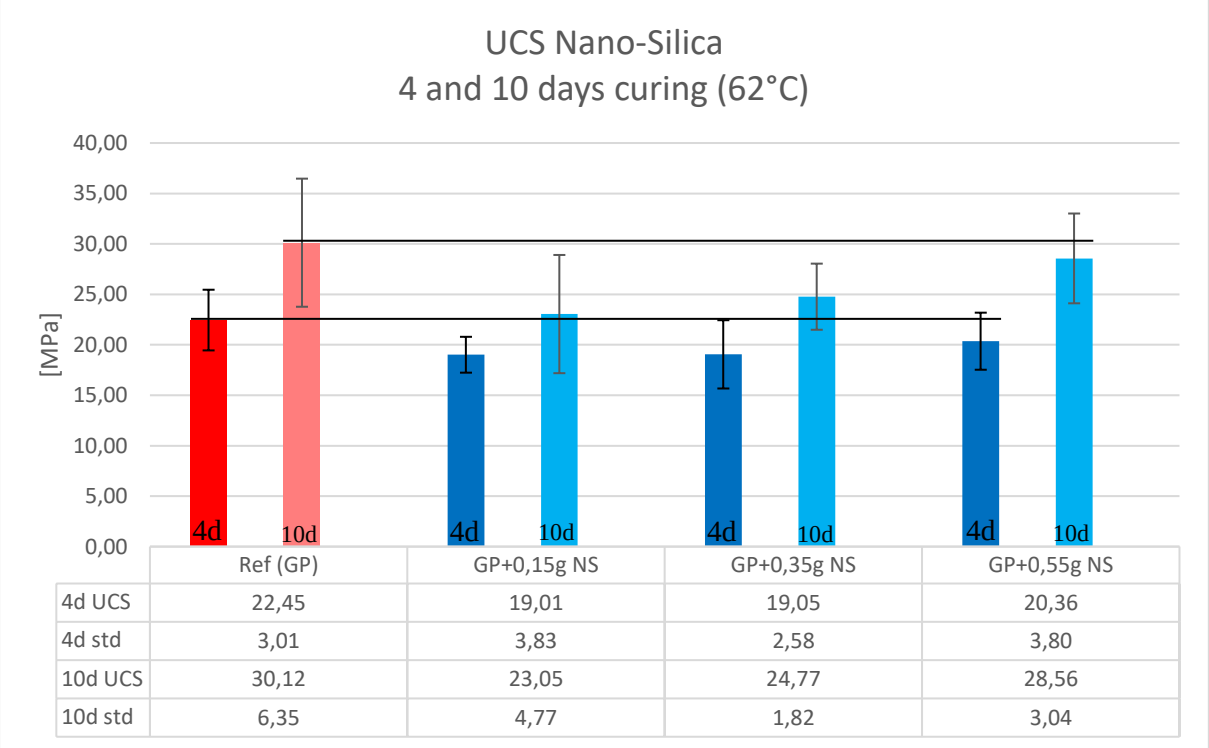

	Ref (GP)	GP+0,15g NS	GP+0,35g NS	GP+0,55g NS
4d UCS	22,45	19,01	19,05	20,36
4d std	3,01	3,83	2,58	3,80
10d UCS	30,12	23,05	24,77	28,56
10d std	6,35	4,77	1,82	3,04

Figure 4. 11 UCS Nano-Silica (NS) after 4 and 10 days of curing

4.4 Further Characterization

Due to time restrictions and using the time available efficiently, further testing of the nano-silica system was performed simultaneously with the UCS testing. Therefore, the nano-silica system was further tested despite showing worse results from UCS than the quartz system.

One of the main tasks for a cementing job in the oil and gas industry is to act as a barrier, to prevent reservoir fluid to reach the surface. NORSOK D-10 also states that cement among others should be impermeable and non-shrinkage. However, if cement does not satisfy these criteria, then the microcracks, high permeability, and porous cement create a leak path for the reservoir fluid. The permeability and shrinkage properties of the plugs are indirectly evaluated through fluid absorption and leakage tests.

Finally, SEM and element analysis are performed to get a better view of the internal properties and structure of the geopolymer.

4.4.1 Fluid Absorption

For fluid absorption, 2 plugs for each mixture were made, including geopolymer reference, 3 steps of nano-silica (0,15g – 0,35g – 0,55g), and OPC. The plugs were cured in the oven at 62° for 7 days and 1 day in air before testing. The plugs before and after polishing can be seen in Figure 4. 12. Since these plugs were not to be tested for UCS, the plugs did not need to have a perfect horizontal surface on top. Therefore, there is no problem that the plugs are a bit uneven, as they are, and this can be seen in Figure 4. 12b).

Figure 4. 12 Plugs for fluid absorption, a) before polishing, b) after polishing

Figure 4. 13 shows the fluid absorption in percent compared to their original weight. The diagram further shows that the geopolymer mixtures with nano-silica had slightly less fluid absorption than the reference and significantly less fluid absorption than OPC. The geopolymers with or without additives absorb significantly less fluid compared to OPC. The effect of nano-silica seems to slightly reduce fluid absorbed, where 0,35g of nano-silica had the lowest.

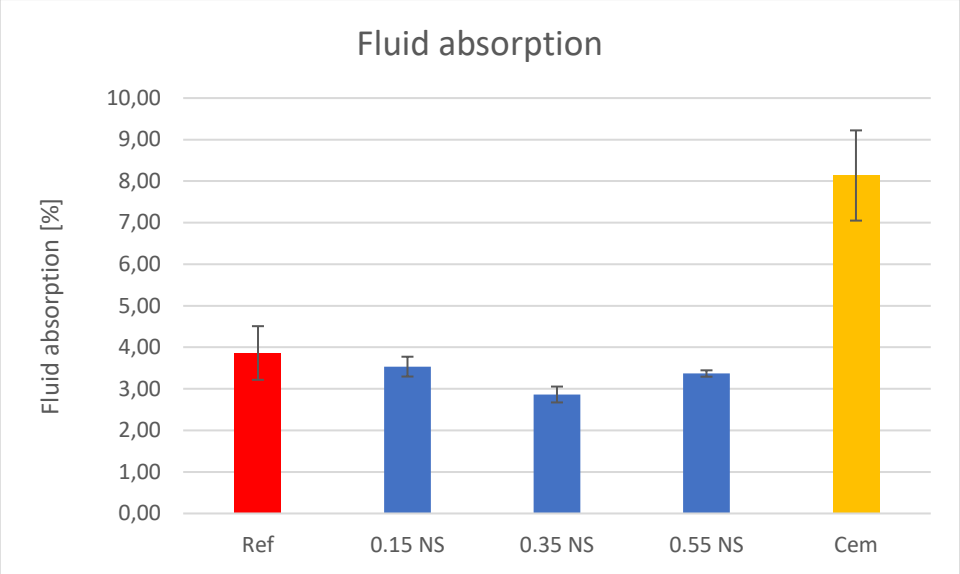

Figure 4. 13 Fluid absorptions in the plugs

4.4.2 Leakage

None of the pipes had any leakage, but a fluid absorption test could also be performed by checking the mass change before and after testing. These results can be seen in Figure 4. 14. Please note that these values are in grams and not a percentage. Since the geopolymer plugs top layer is very porous, and we were unable to remove that because the plugs are set in pipes, it was expected that the results would indicate a higher fluid absorption for geopolymer in this test compared to the previous fluid absorption test. However, this was not the case, results indicate even lower fluid absorption for all geopolymers compared to OPC. The results from fluid absorption from the pipes can indicate that fluid has a harder time penetrating deeper into the geopolymer compared to OPC. Also worth mentioning, this test may not be the most accurate, but results indicate similar findings that were found during fluid absorption testing. Minimal change in fluid absorption between geopolymer mixtures, but significantly less than OPC.

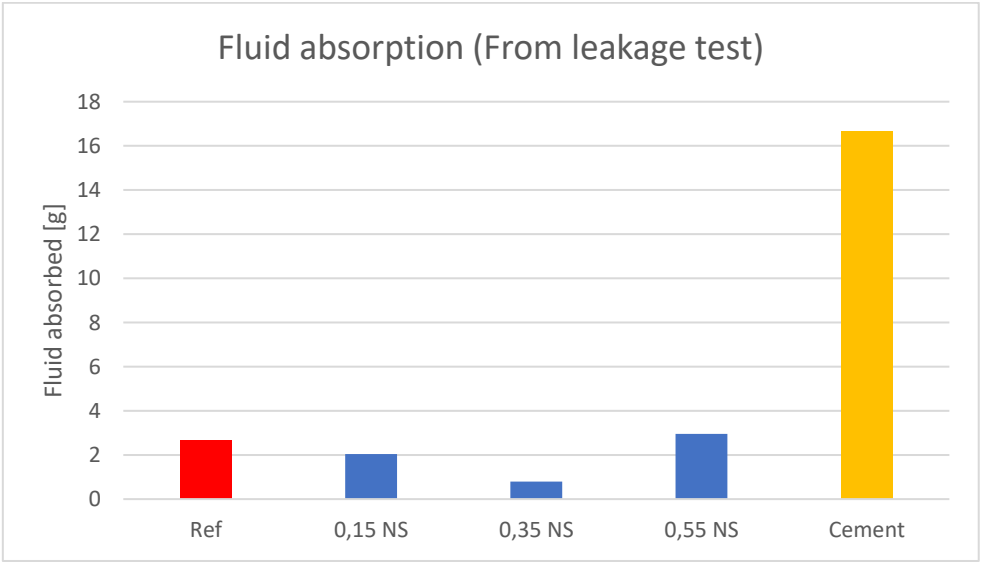

Figure 4. 14 Fluid absorptions of plugs filled in the pipe (leakage)

4.4.3 Rheology

Due to the high amount of fluid transportation in the petroleum industry, the rheology of fluids is a highly important property. For instance, when pumping and circulating cement, the rheological properties are vital to properly calculate the necessary pump pressure and rate, as well as other parameters.

Figure 4. 15 presents the shear stress of the geopolymer with and without nano-silica and for comparison also for OPC. As seen in the graph, there is a significant difference between geopolymer and OPC, but the graph does not show any indication of a difference with the addition of nano-silica. In a practical sense, the difference in rheology for OPC and geopolymer is that geopolymer needs very little force to get it moving from a still state, which acts like water. However, increasing the shear rate increases the shear stress significantly. OPC on the other hand, is relatively thick and starts to gel quickly when still, meaning a higher force is needed to get it moving. Moreover, when increasing the shear rate, the shear stress does increase, but at a much lower rate than for geopolymer.

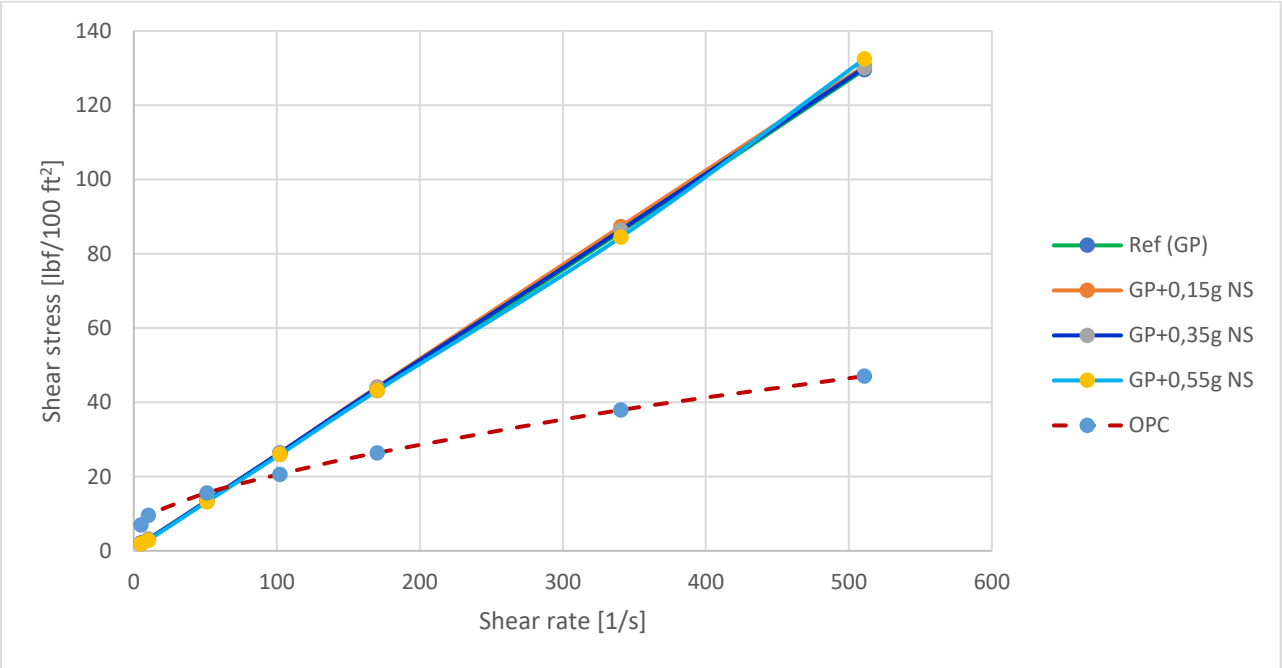

Figure 4. 15 Shear stress of geopolymer slurries and OPC

Looking deeper into the numbers and obtaining Casson plastic viscosity and Casson yield stress, shown in Figure 4. 16 and Figure 4. 17 respectively, the impact of nano-silica on the geopolymer starts to show. The OPC is not included in the diagrams due to the high difference in values making the plots harder to interpret. A high Casson plastic viscosity means that the fluid is more resistant to flow, resulting in creating more friction when flowing. In addition, this means a higher pump pressure is needed to flow adequately. For OPC, the Casson plastic viscosity was approximately one-sixth of the geopolymers, meaning the geopolymer will cause significantly more friction when circulating compared to OPC. On the other hand, a potential benefit of a high Casson plastic viscosity, meaning a thicker fluid, is the ability to carry out

solids from the annulus. The differences seen in Figure 4. 16 are very low, keeping in mind the axis does not start at 0. So, the impact of nano-silica is close to insignificant when it comes to Casson plastic viscosity. Table 4. 2 shows the parameters, including the values for OPC.

Table 4. 2 Rheology parameters

Parameters	OPC	Ref (GP)	GP+0,15 NS	GP+0,35 NS	GP+0,55 NS
τc lbf/100sqft	12,84076	0,11	0,07274	0,07947	0,03126
μc lbf*s^-1/100sqft	0,09120	0,54	0,54701	0,54273	0,55190

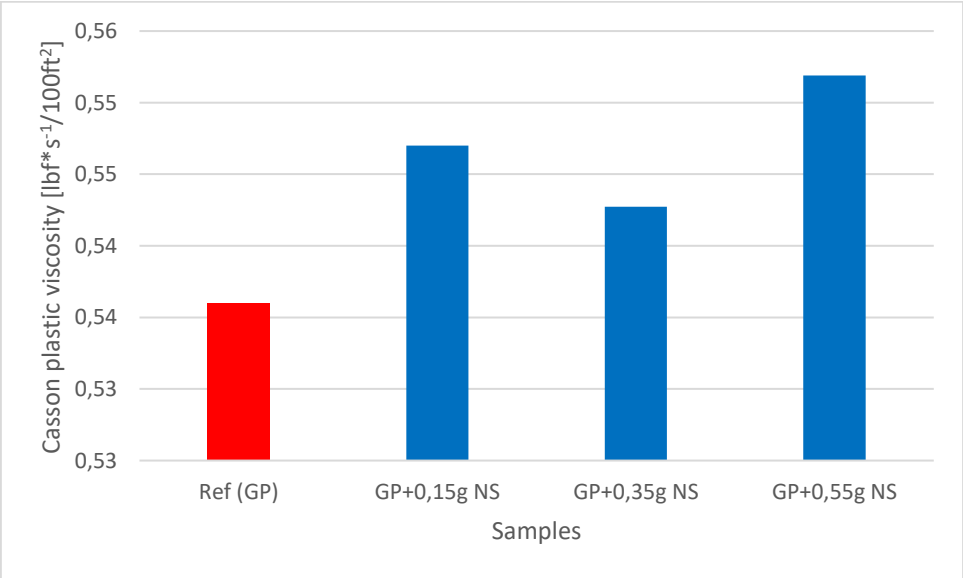

Figure 4. 16 Casson Plastic Viscosity

In Figure 4. 17 the Casson yield strength is presented, and here the difference is noticeable on the diagram. However, the values are very low and close to zero. A lower value indicates less force is required to make the fluid flow. In comparison to OPC, the Casson yield strength is 100 times higher than that of the geopolymer reference.

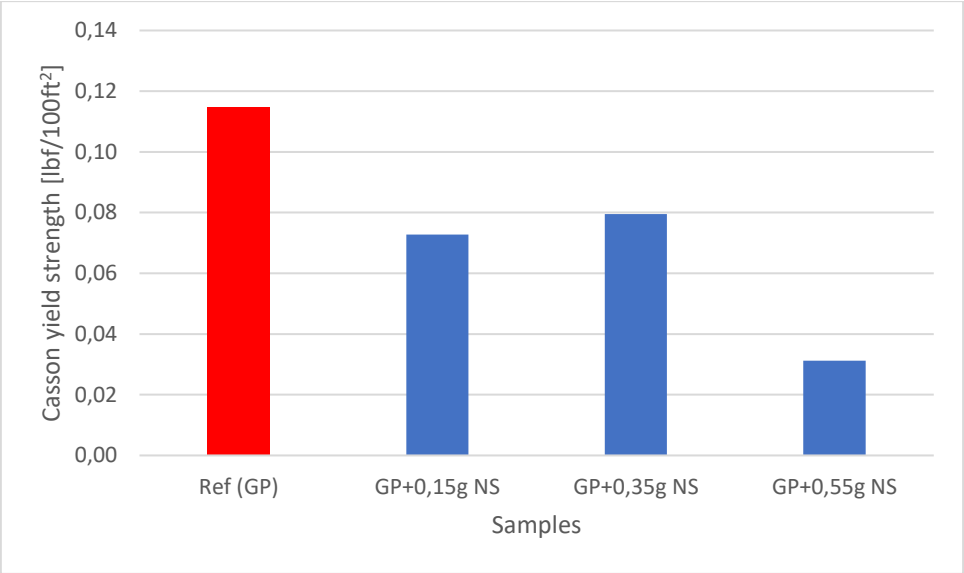

Figure 4. 17 Casson Yield Strength

4.4.4 M-modulus

M-modulus is presented in Figure 4. 18. A high M-modulus value corresponds to a low value for ultrasonic travel time, which in turn indicates that the medium the pulse travels through is of a dense material. A dense medium usually corresponds to a good microstructure, with few significant cracks or pores. Ultimately, a high M-modulus is commonly believed to correlate with a high UCS value.

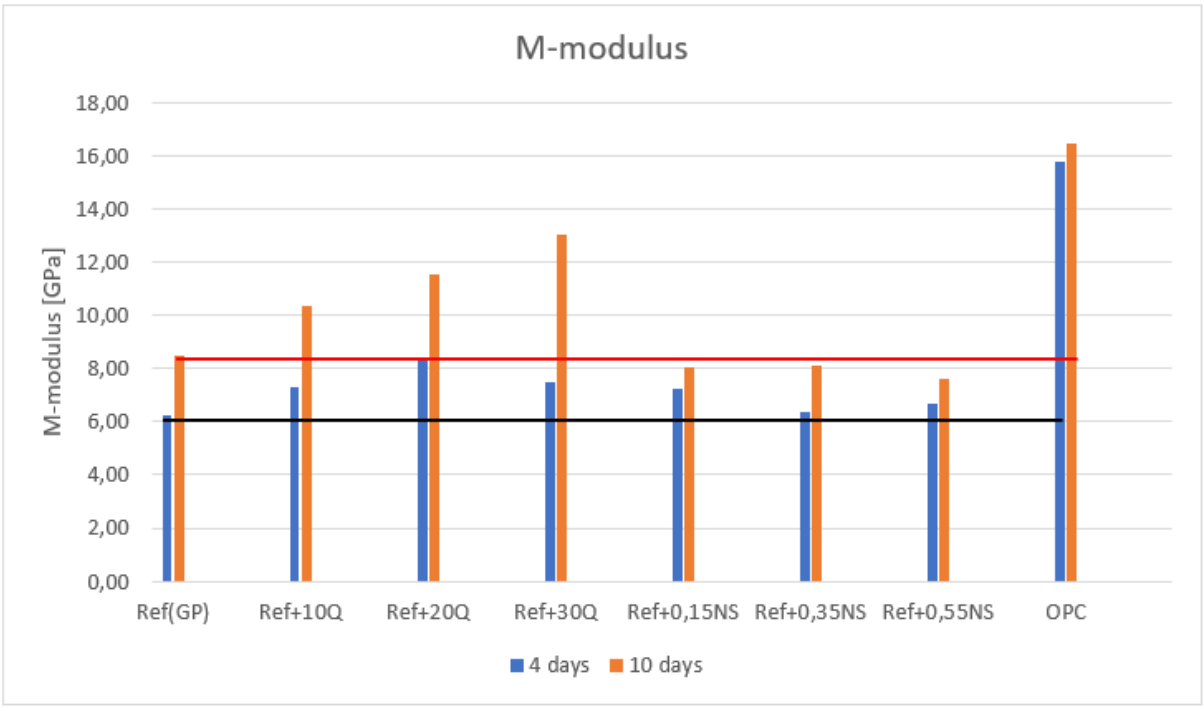

Figure 4. 18 M-modulus

4.4.5 SEM and Element Analysis

For the SEM and element analysis, the remains of 3 plugs after UCS testing were used. All the plugs had 10 days of curing. The plugs used are shown in Table 4. 1.

Table 4. 1 Plugs for SEM and Element Analysis

	Plug number	Curing	Additive
Reference	#3	10 days	None
Quartz	#2	10 days	30g quartz
Nano-Silica	#3	10 days	0,55g nano-silica

Secondary Electron 2 Images (SE2):

The images presented in Figure 4. 19 show the samples with a zoom of 2000x. The balls seen are unreacted fly ash, which means it is desired to have as little of them as possible. Keep in mind that the craters seen, are also indications of unreacted fly ash, but the balls are "on the counterpart/side" of the samples. When comparing the images, there is hard to tell them apart, as there are minor differences, if any. However, one difference spotted is that the amount of unreacted fly ash seems to have increased for the nano-silica system, as there seem to be more balls and craters.

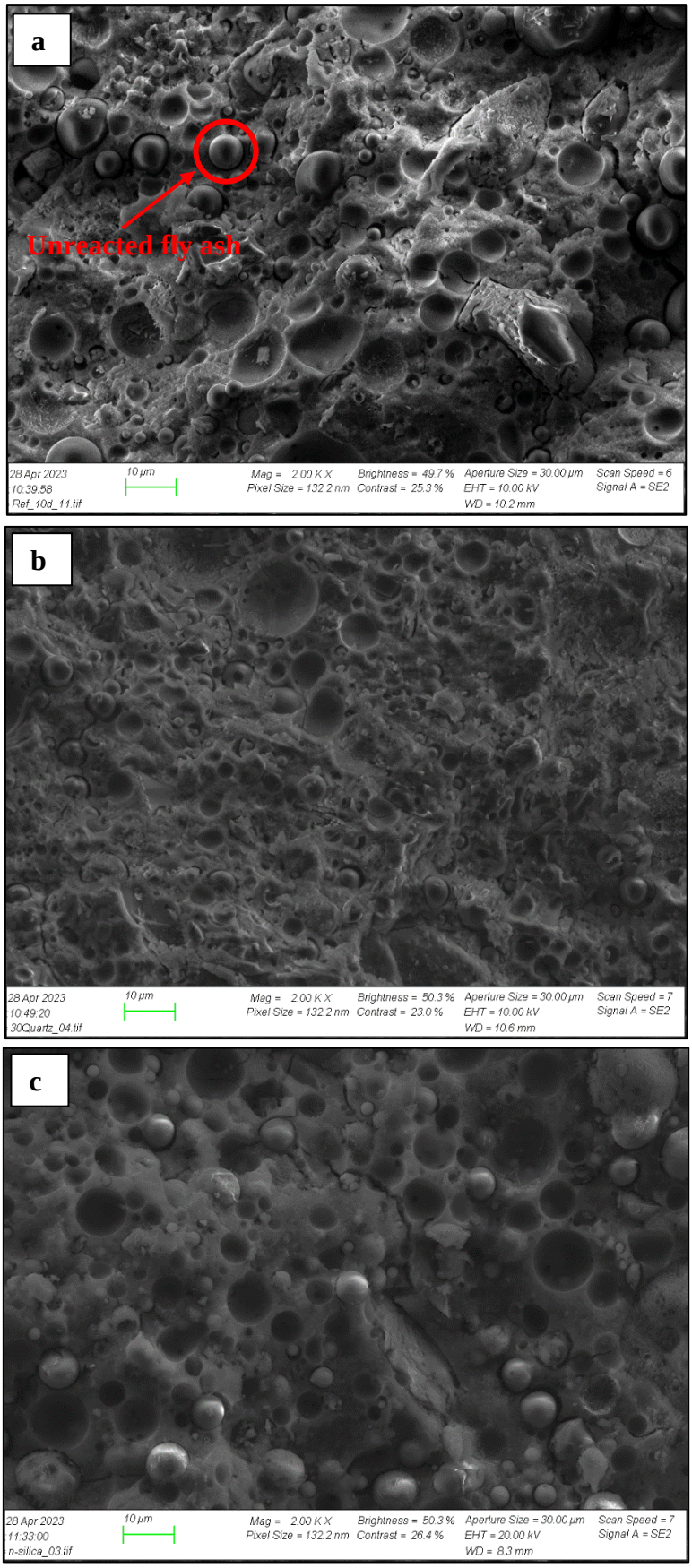

Figure 4. 19 SE2 images for a) Reference, b) Quartz, and c) Nano-Silica

Backscattered Electron Detector Images (BSD):

BSD sends electrons deeper into the samples and gets a better view of the content within. But these images do not show the high-quality resolution of the textures as the SE2 does.

The differences in the images are still minimal and hard to differentiate, but the BSD images did give more indication of the different elements in the samples. Figure 4. 20 presents a BSD image of the reference sample. The images look more "flat" than those of the SE2, but BSD provides more intel, the color grading. The lighter it is, the heavier element is there. As seen in the images, a few white spots appear.

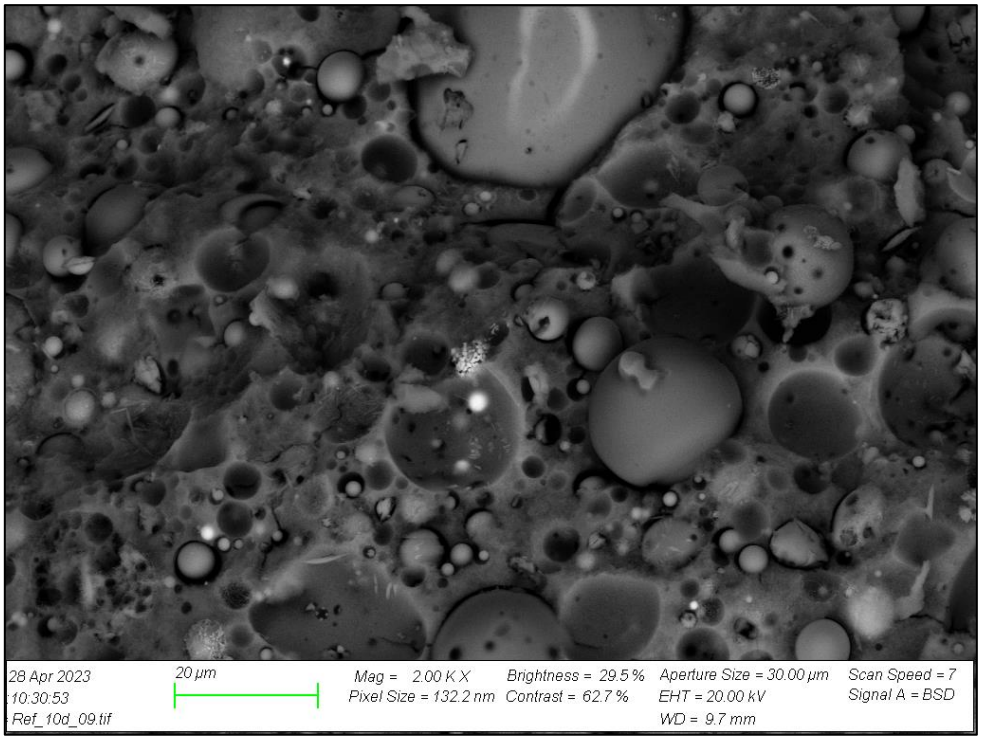

Figure 4. 20 BSD image of Reference (GP)

To further get more information about the structure and better understand these images. Element analyses are taken in "bulk", meaning over a whole area (like over a whole image), and in "spots". These spots chosen are shown in Figure 4. 21, and this is the same image as earlier shown in Figure 4. 20. The spots chosen are one light (EDS Spot 1), one unreacted fly ash spot or "ball" (EDS Spot 2), and lastly of the matrix (EDS Spot 3) to compare to a "normal" area.

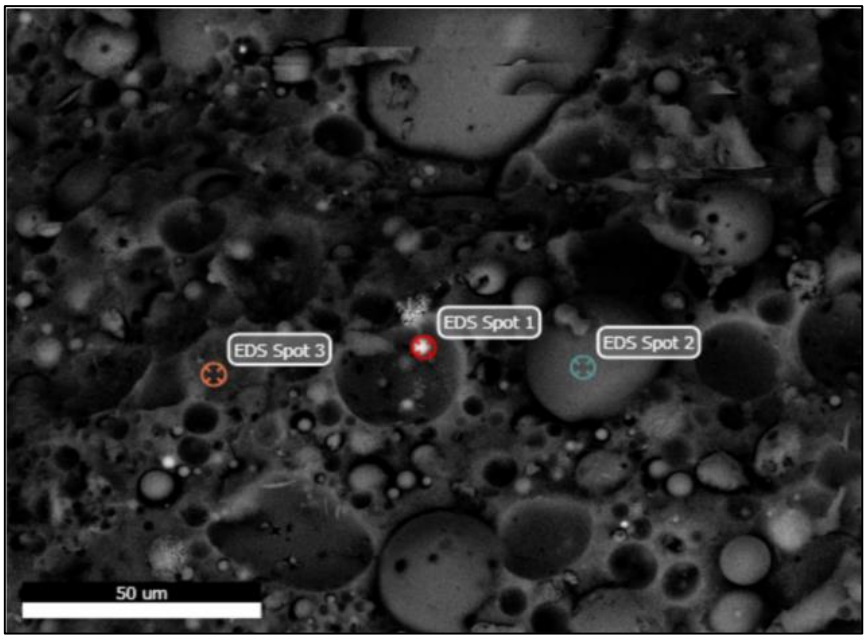

Figure 4. 21 Illustrated spots of "spot"- element analyses

The results of the spot element analysis are shown in Figure 4. 22. The key takeaways compared to spot 3 (matrix):

- Spot 1 (light area) shows a much higher content of iron (Fe), and a less content of silicon (Si).
- Spot 2 (unreacted fly ash/ ball) is fairly similar to the matrix (spot 3) but got a significant increase in the amount of aluminum (Al).

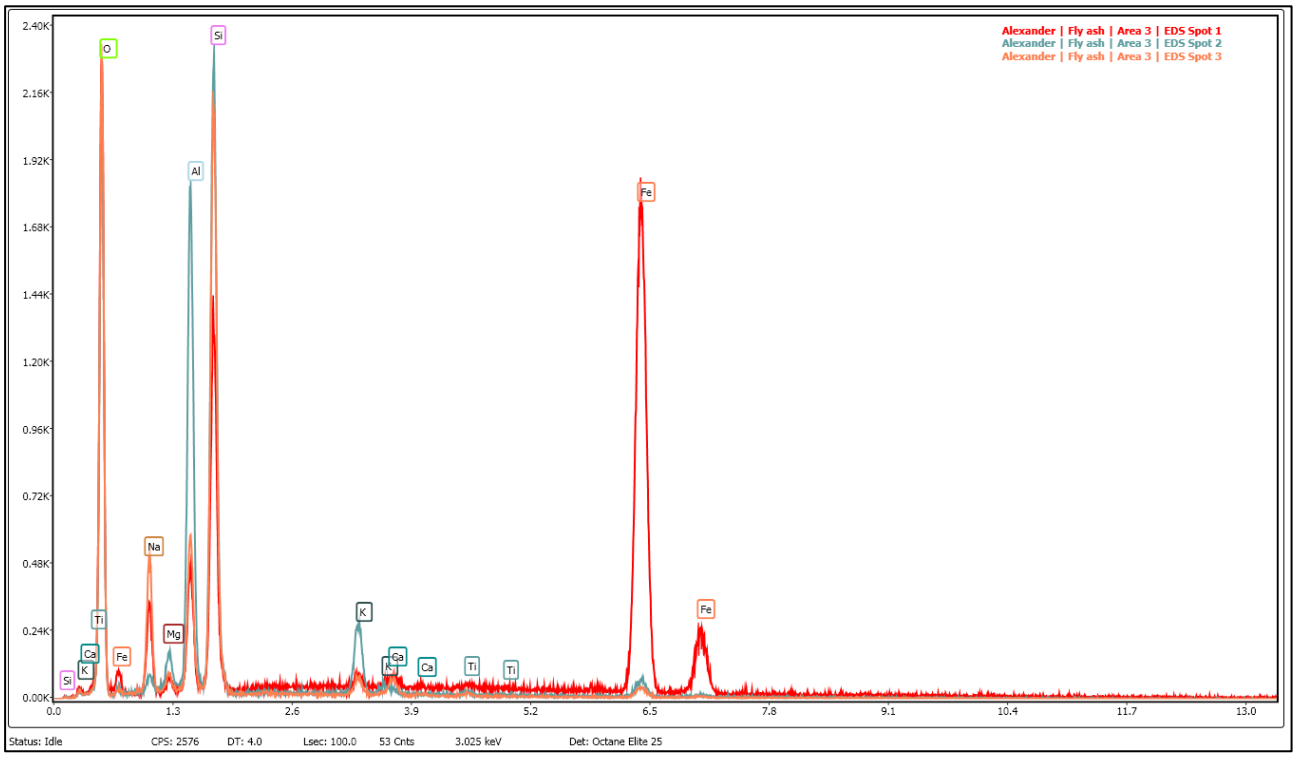

Figure 4. 22 Element spot analysis (Reference)

The "bulk" element analysis is shown in Figure 4. 23.

Figure 4. 23 Bulk Element analysis

More SEM images are found in Appendix C.

4.5 Uncertainties

Slurry preparation: The same procedure was followed for all the slurries, and they were all hand mixed. Air bubbles were attempted removed by gently tapping the plastic cups during and after pouring the slurry. The container used for mixing the slurries was thoroughly cleaned before use, but there is a chance of contamination from previous use. It is also uncertain if all the cement powder was completely dissolved in all slurries during mixing.

Plug preparation: All plugs had to be leveled on top, to make sure they were completely even. This was done by polishing using sandpaper and tested using a spirit leveler for every plug before UCS testing. However, there is still a possibility some plugs were not flat enough, which could result in point load to various degrees, which in turn can result in uneven loading distribution and provide lower results in compressive strength.

Additionally, the top part of the plugs was cut off as these were not representative of the main portion of the plugs. This resulted in different lengths in the plugs, which can impact the UCS results. Therefore, as little as possible was cut off for plugs to UCS testing, and the lengths were thoroughly measured and recorded.

Human error: In general, since all the procedures were conducted by humans, we are likely to make mistakes from time to time, so there is a possibility of human error impacting the experimental results. For example, as mentioned earlier, the fact that the mixing container was hand-cleaned could lead to some contaminations, and the polishing could be imperfect, both could affect the results.

Quantity of experiments: To achieve representative results, the tests were performed multiple times. Due to limited available time, 3 plugs were made per mixture. Then this was later used to average the values as the final results. However, due to some defectiveness or human error, a few outliers were removed from the calculations, leading to an average of 2 plugs instead.

5 Empirical Modelling

This chapter goes into further detail about using the relation between sonic travel time and UCS. There are previous models made to determine the UCS based on their sonic travel time, but these models have been based on different materials like shale and cement. So, as later showed, those models are not very accurate for the geopolymer system. Moreover, new models were made trained on the data from the geopolymer, empirical modeling.

The process of modeling is shown in Figure 5. 1. It starts with a dataset, which is acquired by the empirical data from the UCS and sonic travel time results from the geopolymer. The dataset is then split into two, "Training data" (70% of the dataset) and "Testing data" (30% of the dataset). The model is then trained using only the training data, and for this, two models using regressing were made, Power and Linear. After the model is made, the training data is predicted and compared to the actual/true data. The same is done for the testing data, but keep in mind this data is "unseen" data, meaning the model has not been modeled with this data. Therefore, these results will provide good insight into the accuracy of the model. Lastly, the new models are compared to previous models of others, for both datasets.

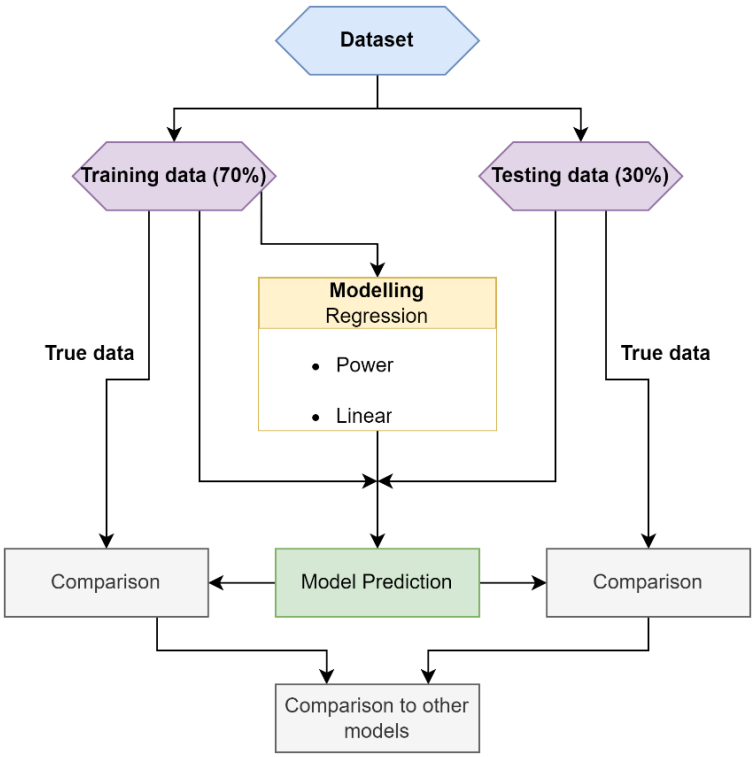

Figure 5. 1 Explanatory modeling flow chart

5.1 New Models Development

As mentioned, the data acquired in the experimental part of this thesis was used to create new models to estimate UCS with the use of sonic velocity, meaning UCS can be determined without conducting destructive testing. The data points used are from the plugs with a curing time of 10 days.

It was also attempted to use the plugs with 4 days of curing, but the data showed no relations, which might be due to the geopolymer had not completed geopolymerization. The data points used are depicted in Figure 5. 2. On the x-axis is the Vp (Sonic travel time) in km/s, and on the y-axis is the UCS in MPa. As the figure displays, the models can be expressed with reasonable accuracy with the linear and power law function, as seen by the R^2 value of 0,6908 and 0,6894 respectively.

Linear model:

Equation 5. 1

$$UCS = 14{,}452Vp - 5{,}0155$$
$$R^2 = 0{,}6908$$

Power law model:

Equation 5. 2

$$UCS = 10{,}453Vp^{1{,}1886}$$
$$R^2 = 0{,}6894$$

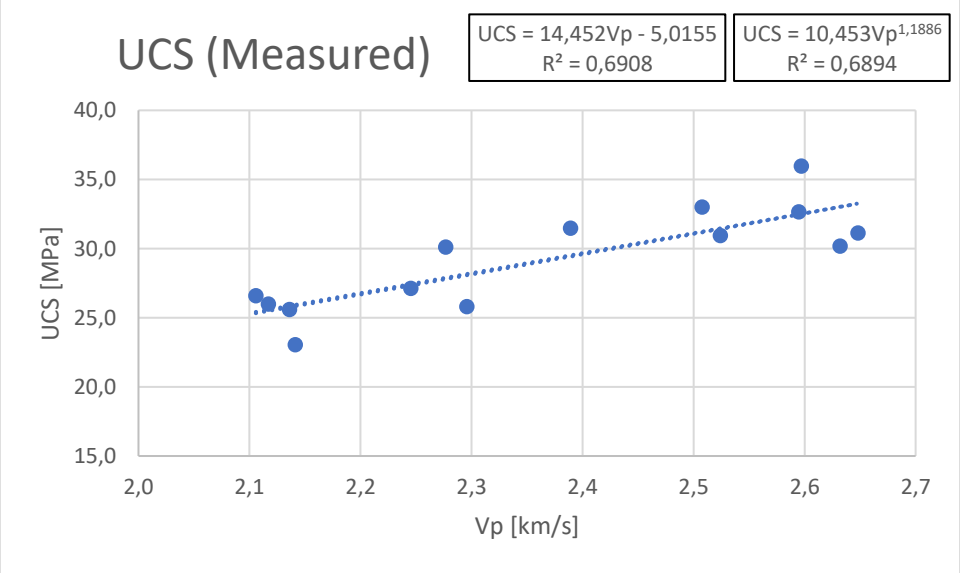

Figure 5. 2 UCS vs Vp

5.2 Comparison of Models

The models are tested and compared using the training data and the testing data, shown in Figure 5. 3 and Figure 5. 4 respectively. The models used to compare are Horsrud's model [35] and Hallvard Titlestad's model [36]. The blue column is the actual UCS results, and the rest are predictions based on the respective models. As seen, both new models made are performing well on both datasets, especially compared to the other models. However, there are commonly in many datapoints deviations, as expected since the R^2 number is not that close to 1. Meaning the new models is unable to predict very accurately but gives reasonable insight into the UCS. Horsrud's model does a slightly better job predicting the UCS than Titlestad's model. This does

not mean that those models are wrong, but they were made and trained on data using different materials. Meaning they work on those systems, not on the geopolymer made in this thesis.

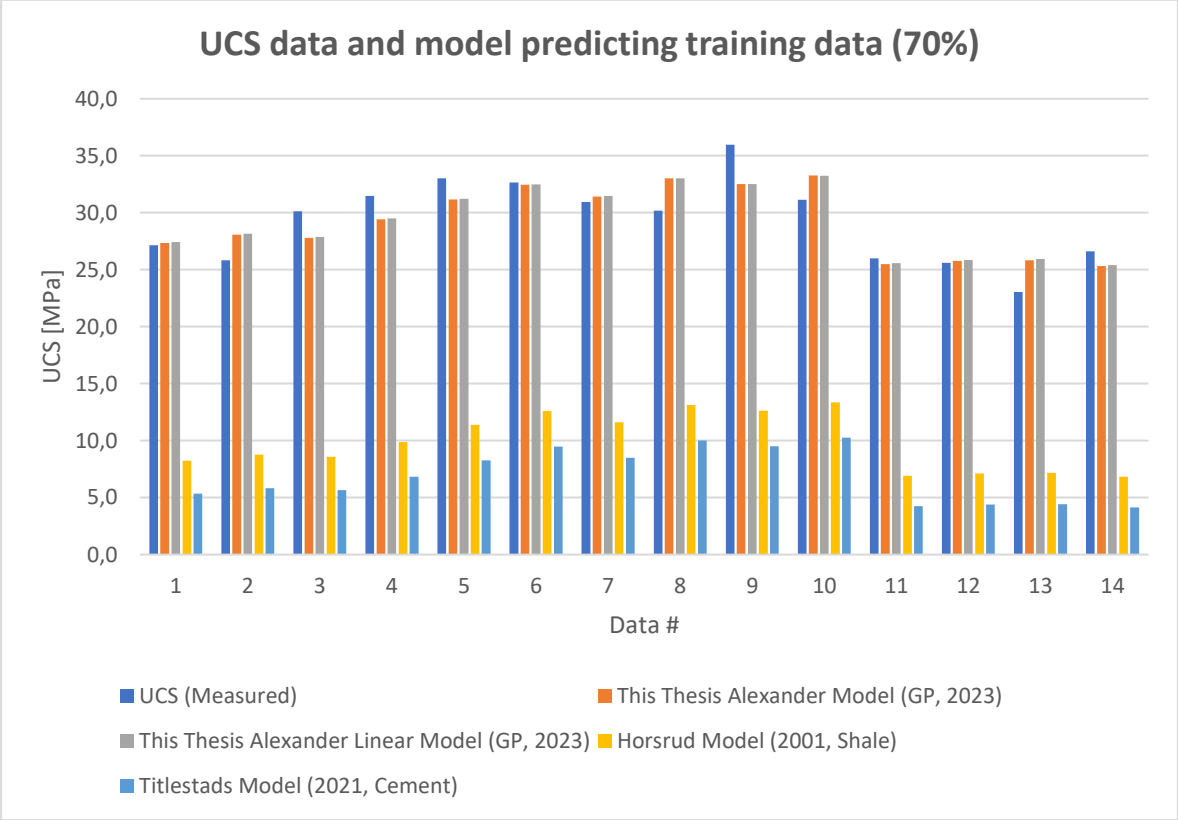

Figure 5. 3 Actual UCS data vs model predictions on training data

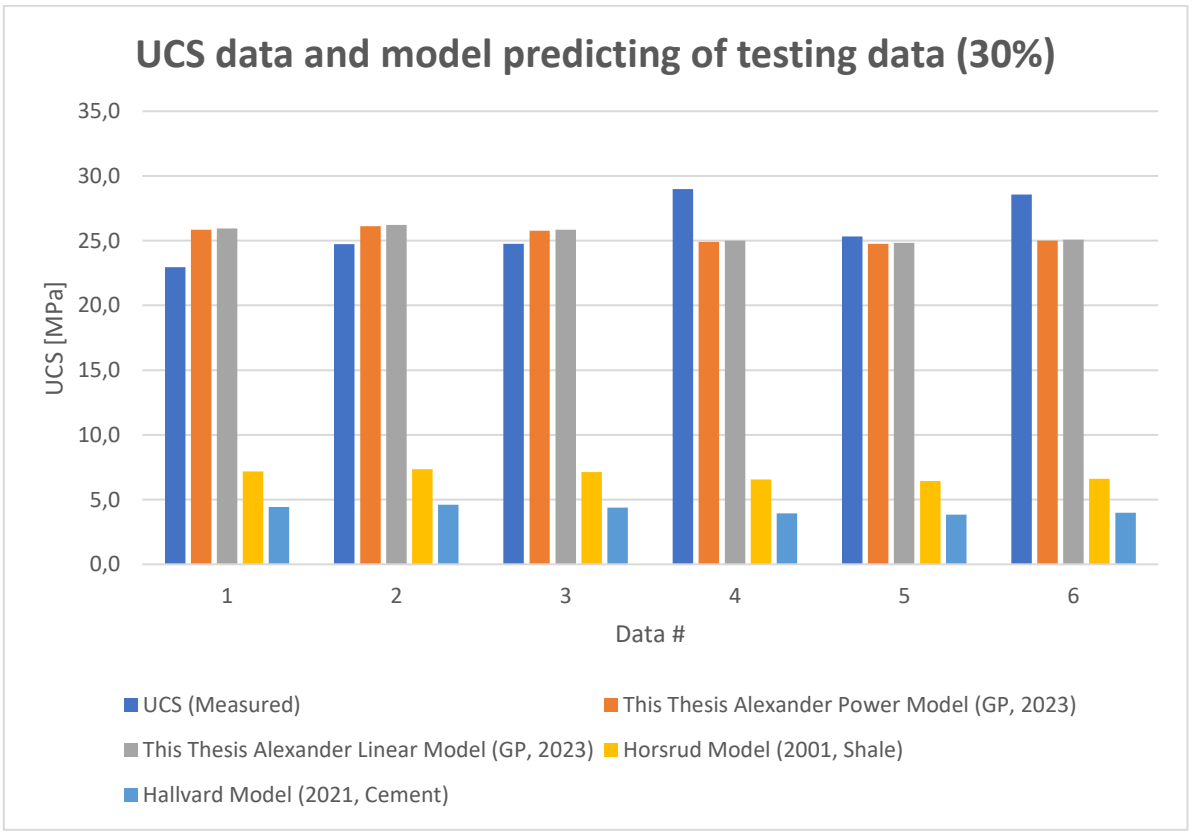

Figure 5. 4 Actual UCS data vs model predictions on testing data

6 Summary and Conclusion

In this thesis, a total of 3 test designs were formulated and tested to investigate the impact of additives on fly-ash-based geopolymer. This section will summarize the experimental works of the best UCS and fluid absorption results and are compared them to the geopolymer reference and OPC. The third last and last columns are colored to represent a positive or negative change in results, whereas red is negative and green positive, as seen in Table 6. 1 and Table 6. 2.

Table 6. 1 Best UCS results from each design

Test Design	Curing time [Days]	Best dosage of additive	Geopolymer (GP)			OPC	
			Ref. Neat GP UCSS [MPa]	Best additive-modified mixture UCS [MPa]	% change with respect to Ref. Neat GP [%]	OPC UCS [MPa]	% change with respect to OPC [%]
Ref. Neat GP	4		22,45			22,72	-1,2 %
	10		30,12			26,02	15,8 %
GP with Quartz	4	10g quartz		23,24	3,5 %		2,3 %
	10	30g quartz		31,13	3,4 %		19,6 %
GP with Nano-Silica (NS)	4	0,55g NS		20,36	-9,3 %		-10,4 %
	10	0,55g NS		28,56	-5,2 %		9,8 %

Table 6. 2 Best fluid absorption results from each design

Test Design	Curing time [Days]	Best dosage of additive	Geopolymer (GP)			OPC	
			Ref. Neat GP UCSS [MPa]	Best additive-modified mixture Fluid Absorption [%]	% change with respect to Ref. Neat GP [%]	OPC Fluid Absorption [%]	% change with respect to OPC [%]
Ref. Neat GP	7	-	3,86	-	-	8,14	-52,6 %
GP with Quartz	N/A						
GP with Nano-Silica (NS)	7	0,35g NS	3,86	2,86	-25,9 %	8,14	-64,9 %

This thesis work summarizes the key observations obtained from the 4 days and 10 days results are as follows:

Geopolymer Reference:

- The newly formulated geopolymer is stronger compared to OPC.
- Exhibited less fluid absorption compared to OPC, which reflects good internal structure and low permeable.

Quartz system:

- The addition of quartz with the given conditions had little effect on UCS.
- More testing should have been performed to determine how over time quartz system behaves.

Nano-Silica:

- During the 4- and 10-days testing time, the addition of nano-silica had a slight negative effect on UCS. This could be the fact that the addition of silica might have reduce the strength development rate. However, overtime, the strength could be different.

- On the other hand, Nano-silica improved the reference even more when it comes to fluid absorption.

Empirical UCS-Vp model:

- The rock and the cement-based literature empirical model did not work for the geopolymer data presented in this thesis.
- The developed empirical model predicted the geopolymer data with reasonable accurate.

SEM and Element Analysis:

- Unreacted fly ash was seen, which may indicate a longer curing time needed, especially for the nano-silica system. This could be the reason the less strength development rate during the 10 days curing time.

Finally, this thesis concludes that the results obtained in this thesis are valid for the considered mixtures concentration and curing conditions. However, they indicate the potential of replacing OPC with geopolymer for application in the oil and gas industry. Even though the quartz and nano silica additives did not show a significant impact on improving the properties of the neat newly formulated geopolymer at the considered curing time and temperature, this thesis suggest investigating the additives impact at different temperature, pressure and curing days such as 14, 21 and 28 days.

7 Future Works

The following suggestions are made for future works:

Exploration of Different Curing Temperature and Durations

While the mixtures analyzed in this study were cured at 62°C, it is worth investigating the effects of alternative curing temperatures, as they may yield different results and provide additional insights. Moreover, extending the curing duration could be beneficial. For instance, an extended curing time of 28 days will reveal more about the long-term performance of the materials.

Expansions of the Sample Size

In this study, the sample size comprised of three plugs. Increasing the sample size in future studies can bolster the reliability of the results by reducing statistical uncertainties and enhancing the overall accuracy.

Increase the Concentration of Quartz

Future work could delve into the effects of increasing the quartz concentration in the mixture. It would be intriguing to discern the implications of this modification on the material's properties. Furthermore, varying the particle size of quartz could also shed light on its impact on the mixture's performance.

Increase the Concentration of Nano-Silica

Similarly, studies focusing on the impact of higher concentrations of nano-silica could be equally enlightening. Such research could contribute to a deeper understanding of the role nano-silica plays in the mixture.

Integration of Optimal Mixtures

The potential synergistic effects resulting from the combined addition of both quartz and nano-silica merit exploration. The emergence of a new optimal mixture through this combination could be a significant breakthrough.

Enhancement of Leakage Testing

The leakage test conducted in this study presented some limitations. A more advanced approach for future research could be to perform a pressurized leakage test. Having pressure on the side of the fluid and monitor any resultant leakage. This technique could lead to a more accurate and comprehensive assessment of leakage performance.

8 References

[01]. (n.d.). *PetroWiki*. Retrieved from PetroWiki Cementing operations: https://petrowiki.spe.org/index.php?title=Cementing_operations&oldid=53699

[02] Salami, O. (2014). Synthesis and Working Mechanism of Himic Acid Graft Copolymer Fluid Loss Additives Suitable for Cementing High Pressure/High Temeprature oil and Gas Wells. *Munchen: TECHNISCHE UNIVERSITAT MUNCHEN*.

[03] Vrålstad, T., Saasen, A., Fjær, E., Øia, T., Ytrehus, J. D., & Khalifeh, M. (2019, February). Plug & abandonment of offshore wells: Ensuring long-term well integrity and cost-efficiency. *Journal of Petroleum Science and Engineering*, pp. 478-491. doi:10.1016/j.petrol.2018.10.049

[04] Stokes, D. (2017, May 9). *Integrated milling, underreaming approach streamlines P&A operations in the North Sea*. Retrieved from Offshore-mag.com: https://www.offshore-mag.com/drilling-completion/article/16756041/integrated-milling-underreaming-approach-streamlines-pa-operations-in-the-north-sea

[05]. (2021). *NORSOK D-010 Well integrity in drilling and well drilling operations, rev 5.* Standards Norway.

[06] Vignes, B., & Aadnøy, B. S. (2009, October 28). Well-Integrity Issues Offshore Norway. *OnePetro*. doi:10.2118/112535-PA

[07]. (2015, June 25). *Cement composition and classification*. Retrieved from PetroWiki: https://petrowiki.spe.org/Cement_composition_and_classification

[08], Prisca, S., & Mahmood, A. (2013). SPECIAL CONSIDERATIONS IN CEMENTING HIGH PRESSURE HIGH TEMPERATURE WELLS. 143 2012 EAAS & ARF. *International Journal of Engineering and Applied Sciences*.

[09], Nelson, E. B., & Guillot, D. (2006, June 28). Well Cementing. Retrieved from https://www.slb.com/resource-library/book/well-cementing

[10] Broni-Bediako., E. (2150). Evaluation of the Performance of Local Cements with Imported Class 'G' Cement for Oil Well Cementing Operations in Ghana. *Ghana Mining Journal (GMJ)*, pp. 78-84.

[11], Teodoriu, C., Yi, M. C., & Salehi, S. (2019, September 5). A Novel Experimental Investigation of. *MDPI Energies 2019*. doi:10.3390/en12183426

[12] Aleem, M. A., & Arumairaj, P. (2012). Optimum mix for the geopolymer concrete. *Indian Journal of Science and Technology*, pp. 1-3. doi:10.17485/ijst/2012/v5i3.8

[13] Naskar, S., & Chakraborty, A. K. (2016, September). Effect of nano materials in geopolymer concrete. *Perspectives in Science*, pp. 273-275. doi:10.1016/j.pisc.2016.04.049

[14] Han, Q., Zhang, P., Wu, J., Jing, Y., Zhang, D., & Zhang, T. (2022, April). Comprehensive review of the properties of fly ash-based geopolymer with additive of nano-SiO2. *Nanotechnology Reviews*. doi:10.1515/ntrev-2022-0092

[15] Assaedi, H., Alomayri, T., Kaze, C. R., Jindal, B. B., Subaer, S., Shaikh, F., & Alraddadi, S. (2020, August). Characterization and properties of geopolymer nanocomposites with different contents of nano-CaCO3. *Construction and Building Materials*. doi:10.1016/j.conbuildmat.2020.119137

[16] Alvi, M. A., Khalifeh, M., & Agonafir, M. B. (2020, August). Effect of nanoparticles on properties of geopolymers designed for well cementing applications. *Journal of Petroleum Science and Engineering*. doi:10.1016/j.petrol.2020.107128

[17] Duan, P., Yan, C., Luo, W., & Zhou, W. (2016, March). Effects of adding nano-TiO2 on compressive strength, drying shrinkage, carbonation and microstructure of fluidized bed fly ash based geopolymer paste. *Construction and Building Materials*, pp. 115-125. doi:10.1016/j.conbuildmat.2015.12.095

[18] Rahmawati, C., Aprilia, S., Saidi, T., Aulia, T. B., & Hadi, A. E. (2021, June). The Effects of Nanosilica on Mechanical Properties and Fracture Toughness of Geopolymer Cement. *Geopolymer Composite*. doi:10.3390/polym13132178

[19] Deb, P. S., Sarker, P. K., & Barbhuiya, S. (2015, December). Effects of nano-silica on the strength development of geopolymer cured at room temperature. *Construction and Building Materials*, pp. 675-683. doi:10.1016/j.conbuildmat.2015.10.044

[20] Zidi, Z., Ltifi, M., & Zafar, I. (2021, January). Synthesis and attributes of nano-SiO2 local metakaolin based-geopolymer. *Journal of Building Engineering*. doi:10.1016/j.jobe.2020.101586

[21] Phoo-ngernkham, T., Chindaprasirt, P., Sata, V., Hanjitsuwan, S., & Hatanaka, S. (2014, March). The effect of adding nano-SiO2 and nano-Al2O3 on properties of high calcium fly ash geopolymer cured at ambient temperature. *Materials & Design*, pp. 58-65. doi:doi.org/10.1016/j.matdes.2013.09.049

[22]. (n.d.). *Heidelberg Materials*. Retrieved from https://www.sement.heidelbergmaterials.no/no

[23]. (n.d.). *Sodium hydroxide 98.5-100.5%, pellets, AnalaR NORMAPUR® Reag. Ph. Eur. analytical reagent*. Retrieved from VWR Chemicals: https://cz.vwr.com/store/product/en/781220/sodium-hydroxide-98-5-100-5-pellets-analar-normapur-reag-ph-eur-analytical-reagent

[24] Mavko, G., Mukerji, T., & Dvorkin, J. (2010). *The Rock Physics Handbook.* Tools for Seismic Analysis of Porous Media, Cambridge University Press.

[25] Nelson, E., & Guillot, D. (2006). *Well Cementing, Second Edition.* Schlumberger.

[26] Fjær, E., Holt, R., Horsrud, P., & Raaen, A. (2008). *Petroleum Related Rock Mechanics, Second Edition.* Elsevier Science.

[27] Purdue University. (n.d.). *Scanning Electron Microscope - Radiological and Environmental Management*. Retrieved April 2023, from Purdue.edu: https://www.purdue.edu/ehps/rem/laboratory/equipment%20safety/Research%20Equipment/sem.html

[28] Jamieson, E., McLellan, B., Riessen, A. v., & Nikraz, H. (2015, July 15). Comparison of embodied energies of Ordinary Portland Cement with Bayer-derived geopolymer products. *Journal of Cleaner Production*, pp. 112-118. doi:10.1016/j.jclepro.2015.03.008

[29] Hardjito, D., Wallah, S. E., Sumajouw, D. M., & Rangan, B. (2004, 1 11). On the Development of Fly Ash-Based Geopolymer Concrete. *Materials Journal*, pp. 467-472. doi:10.14359/13485

[30] Adam, A. A. (2019, May). The Effects of Water to Solid Ratio, Activator to Binder Ratio, and Lime Proportion on the Compressive Strength of Ambient-Cured Geopolymer Concrete. *Journal of the Civil Engineering Forum*. doi:10.22146/jcef.43878

[31] Pendse, D., & Chin, A. (2001). Cathodoluminescence and Transmission Cathodoluminescence. *Encyclopedia of Materials: Science and Technology*, pp. 1-7. doi:10.1016/B0-08-043152-6/00190-X

[32] Ng, H., Heah, C., Liew, Y., & Abdullah, M. (2018, December). The Effect of Various Molarities of. *AIP Conference Proceedings*. doi:10.1063/1.5080911

[33] Hamidi, R. M., Man, Z., & Azizli, K. A. (2016). Concentration of NaOH and the Effect on the Properties of Fly Ash Based Geopolymer. *Elsevier, Procedia Engineering*, ss. 189-193. doi:10.1016/j.proeng.2016.06.568

[34]. (n.d.). *Nyacol Nano Technologies, Inc.* Retrieved from https://www.nyacol.com/

[35] Horsrud, P. (2001, June). Estimating Mechanical Properties of Shale From Empirical Correlations. *SPE Drill. Complet., vol. 16, no. 02*. doi:10.2118/56017-PA

[36] Titlestad, H. (2021). *Effect of nano-SiO2 , nano-Al2O3 , MWCNT and FA on properties of Portland G-class cement.* MSc Thesis University of Stavanger.

[37]. (u.d.). *Merck*. Hentet fra Sigmaaldrich: https://www.sigmaaldrich.com/NO/en

9 Appendix A – Measured and Calculated Dataset

Appendix A contains raw data like length, mass, etc. obtained before and after destructive testing of the specimens.

4 days in the oven (62°C)

Plug	Mass [g]	Diameter [mm]	Length [mm]	Volume [m^3]	Density [kg/m^3]	Sonic [µs]	Vp [m/s]	Modulus of Elasticity (M) [Gpa]	UCS (Max Load) [N]	UCS [MPa]
Ref (GP) #1	85,2	32,8	59,9	5,06E-05	1683	31,2	1920	6,2	21,3	25
Ref (GP) #2	85,2	32,8	60,2	5,09E-05	1675	31,0	1942	6,3	16,3	19
Ref (GP) #3	85,2	32,8	60,4	5,10E-05	1669	31,5	1917	6,1	19,3	23
Ref+10Q #1	86,7	32,8	56,3	4,76E-05	1823	27,7	2032	7,5	19,7	23
Ref+10Q #2	86,7	32,8	56,3	4,76E-05	1823	28,0	2011	7,4	21,1	25
Ref+10Q #3	87,0	32,8	56,4	4,77E-05	1826	28,7	1965	7,1	18,1	21
Ref+20Q #1	85,7	32,8	54,9	4,64E-05	1847	25,8	2128	8,4	18,1	21
Ref+20Q #2	87,0	32,8	55,9	4,72E-05	1842	26,8	2086	8,0	12,6	15
Ref+20Q #3	87,1	32,8	55,9	4,72E-05	1844	26,1	2142	8,5	14,0	17
Ref+30Q #1	85,0	32,8	55,3	4,67E-05	1819	27,4	2018	7,4	17,7	21
Ref+30Q #2	83,2	32,8	54,5	4,61E-05	1807	26,1	2088	7,9	16,1	19
Ref+30Q #3	84,0	32,8	54,9	4,64E-05	1811	27,7	1982	7,1	13,0	15
Ref+0,15NS #1	82,1	32,8	57,6	4,87E-05	1687	27,4	2102	7,5	13,5	16
Ref+0,15NS #2	84,6	32,8	58,1	4,91E-05	1723	28,6	2031	7,1	19,7	23
Ref+0,15NS #3	83,1	32,8	58,0	4,90E-05	1696	28,1	2064	7,2	15,0	18
Ref+0,35NS #1	84,7	32,8	59,0	4,99E-05	1699	30,7	1922	6,3	14,6	17
Ref+0,35NS #2	84,6	32,8	58,1	4,91E-05	1723	30,2	1924	6,4	18,6	22
Ref+0,35NS #3	86,2	32,8	59,3	5,01E-05	1720	30,7	1932	6,4	15,1	18
Ref+0,55NS #1	87,4	32,8	60,3	5,10E-05	1715	30,3	1990	6,8	16,4	19
Ref+0,55NS #2	89,2	32,8	59,8	5,05E-05	1765	30,3	1974	6,9	20,3	24
Ref+0,55NS #3	89,7	32,8	60,2	5,09E-05	1763	31,2	1929	6,6	15,6	18
Ref+0,55NS #4	88,7	32,8	59,7	5,04E-05	1758	31,3	1907	6,4	20,6	24
Ref+0,55NS #5	88,9	32,8	61,2	5,17E-05	1719	30,8	1987	6,8	13,1	16
Cem #1	95,0	32,8	64,3	5,43E-05	1749	21,3	3019	15,9	20,4	24
Cem #2	93,6	32,8	63,4	5,36E-05	1747	21,2	2991	15,6	17,6	21
Cem #3	86,0	32,8	58,4	4,93E-05	1743	19,4	3010	15,8	19,6	23

7 days in the oven (62°C)

Plug	Mass [g]	Diameter [mm]	Length [mm]	Volume [m^3]	Density [kg/m^3]	Sonic [µs]	Vp [m/s]	Modulus of Elasticity (M) [Gpa]	UCS (Max Load) [N]	UCS [MPa]
Ref (GP) #1	84,7	32,8	60,6	5,12E-05	1655	27,6	2195	8,0	26,7	32
Ref (GP) #2	85,1	32,8	60,7	5,13E-05	1659	27,5	2208	8,1	30,0	35
Ref (GP) #3	83,7	32,8	60,2	5,08E-05	1646	27,6	2180	7,8	24,8	29

10 days in the oven (62°C)

Plug	Mass [g]	Diameter [mm]	Length [mm]	Volume [m^3]	Density [kg/m^3]	Sonic [µs]	Vp [m/s]	Modulus of Elasticity (M) [Gpa]	UCS (Max Load) [N]	UCS [MPa]
Ref (GP) #1	79,1	32,8	57,3	4,84E-05	1635	25,5	2245	8,2	22,9	27
Ref (GP) #2	79,2	32,8	57,2	4,84E-05	1638	25,0	2289	8,6	31,6	37
Ref (GP) #3	78,6	32,8	56,9	4,81E-05	1634	24,8	2296	8,6	21,8	26
Ref+10Q #1	76,9	32,8	51,5	4,35E-05	1767	21,4	2407	10,2	10,0	12
Ref+10Q #2	82,6	32,8	55,0	4,65E-05	1777	22,7	2423	10,4	19,6	23
Ref+10Q #3	80,5	32,8	52,8	4,46E-05	1804	22,1	2389	10,3	26,6	31
Ref+20Q #1	77,2	32,8	49,9	4,22E-05	1831	19,9	2508	11,5	27,9	33
Ref+20Q #2	75,6	32,8	49,3	4,17E-05	1815	19,0	2595	12,2	27,6	33
Ref+20Q #3	72,6	32,8	48,4	4,09E-05	1775	19,6	2469	10,8	23,0	27
Ref+30Q #1	75,5	32,8	47,9	4,05E-05	1865	18,2	2632	12,9	25,5	30
Ref+30Q #2	79,2	32,8	50,5	4,27E-05	1856	18,6	2715	13,7	23,0	27
Ref+30Q #3	77,8	32,8	49,6	4,19E-05	1856	19,1	2597	12,5	30,4	36
Ref+0,15NS #1	79,2	32,8	53,4	4,51E-05	1755	24,6	2171	8,3	14,8	18
Ref+0,15NS #2	77,3	32,8	52,5	4,44E-05	1743	24,8	2117	7,8	22,0	26
Ref+0,15NS #3	79,0	32,8	53,4	4,51E-05	1751	25,0	2136	8,0	21,6	26
Ref+0,35NS #1	79,6	32,8	51,8	4,38E-05	1819	24,6	2106	8,1	22,5	27
Ref+0,35NS #2	78,7	32,8	52,9	4,47E-05	1761	24,7	2142	8,1	19,4	23
Ref+0,35NS #3	77,7	32,8	52,5	4,44E-05	1752	24,3	2160	8,2	20,9	25
Ref+0,55NS #1	78,2	32,8	52,9	4,47E-05	1749	25,1	2108	7,8	26,5	31
Ref+0,55NS #2	76,2	32,8	51,5	4,35E-05	1751	24,8	2077	7,6	24,5	29
Ref+0,55NS #3	79,7	32,8	54,1	4,57E-05	1744	26,2	2065	7,4	21,4	25
Cem #1	95,2	32,8	66,2	5,59E-05	1702	20,2	3277	18,3	21,4	25
Cem #2	93,2	32,8	65,9	5,57E-05	1674	21,6	3051	15,6	25,0	30
Cem #3	92,9	32,8	65,6	5,54E-05	1676	21,6	3037	15,5	19,6	23

Viscosity readings

Rpm	300	200	100	60	30	6	3
Ref (GP)	270	179	90	55	28	6,5	4,4
Ref+0,15NS	272	182	92	55	28	6,5	4
Ref+0,35NS	271	180	91,5	55	28	6,5	4
Ref+0,55NS	276	176	90	54	27,5	6	4
Cem	98	79	55	43	32,5	20	14,5
Ref+Quartz	Not Tested						

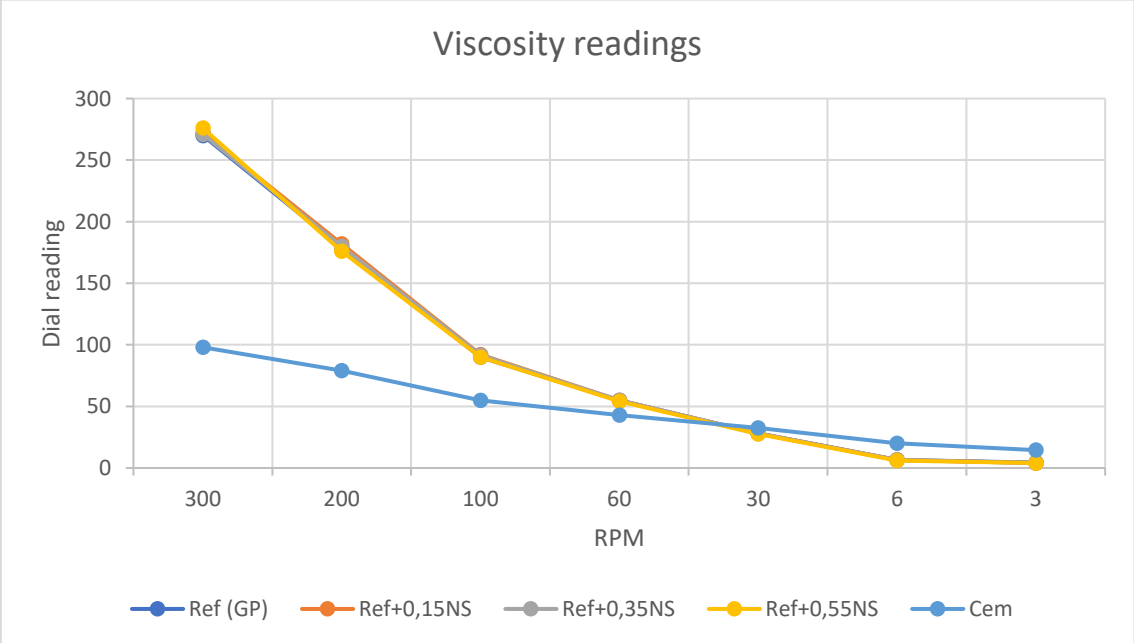

Fluid absorption

	Mass [g]	Delta Mass (24h) [g]	Delta Mass (48h) [g]	Delta Mass (72h) [g]	Delta Mass after 3 days [g]	Delta mass [%]
Ref (GP) #1	77,5	2,76	-0,04	-0,08	2,64	3,4
Ref (GP) #2	75,7	3,56	-0,23	-0,06	3,27	4,3
Ref+0,15NS #1	76,93	2,67	0	-0,08	2,59	3,4
Ref+0,15NS #2	76,14	2,98	-0,14	-0,02	2,82	3,7
Ref+0,35NS #1	78,79	2,3	-0,06	-0,09	2,15	2,7
Ref+0,35NS #2	77,02	2,51	-0,13	-0,07	2,31	3,0
Ref+0,55NS #1	77,22	2,7	-0,1	-0,04	2,56	3,3
Ref+0,55NS #2	77,69	2,84	-0,1	-0,08	2,66	3,4
Cem #1	76,41	4,51	1	0,12	5,63	7,4
Cem #2	73,9	6,11	0,26	0,21	6,58	8,9

Quartz particle size distribution

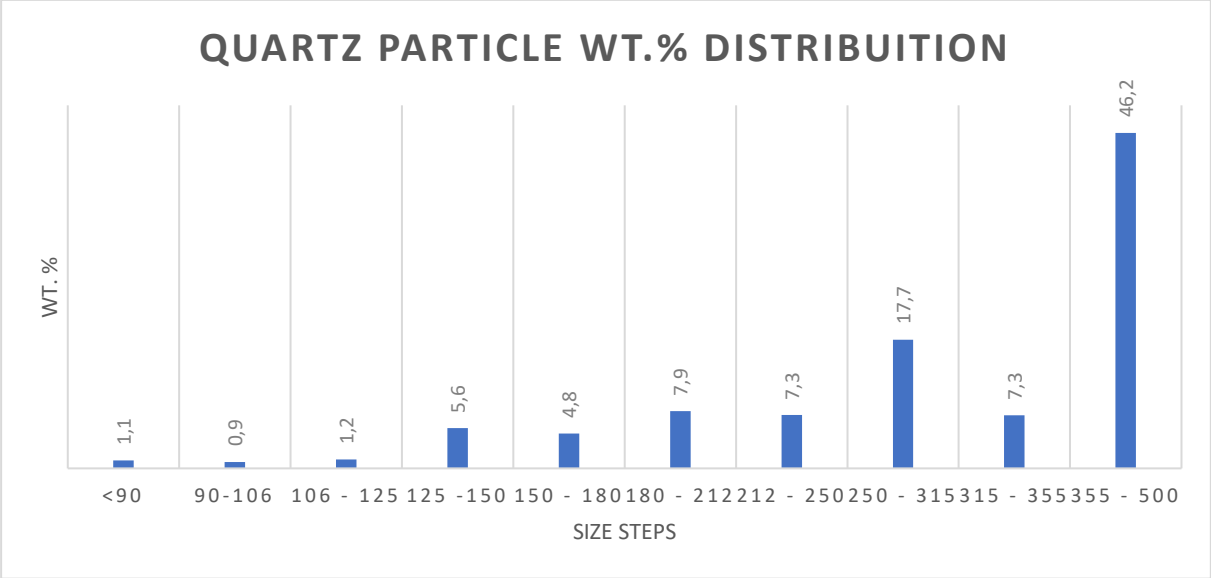

10 Appendix B – Testing History

Description	Start date	End date	Duration [d]
First viscosity test	06.mar	06.mar	1
Curing test (62C and 105C)	06.mar	11.mar	6
Ref UCS (4d)	06.mar	13.mar	8
Quartz UCS (4d)	10.mar	17.mar	8
Ref UCS (7d and 10d)	14.mar	26.mar	13
Quartz UCS (10d)	18.mar	30.mar	13
Cement Leakage	19.mar	01.apr	14
Cement UCS (10d)	19.mar	31.mar	13
Study trip	20.mar	27.mar	8
Nano UCS (10d)	31.mar	12.apr	13
Ref, Nano, Cement full viscosity	01.apr	01.apr	1
Ref, Nano, Cement Fluid absorp	01.apr	13.apr	13
Ref and Nano Leakage	01.apr	19.apr	19
Nano UCS (4d)	02.apr	09.apr	8
New leakage for Nano 0,55	02.apr	20.apr	19
Cement UCS (4d)	10.apr	17.apr	8
SEM and element analysis	28.apr	28.apr	1

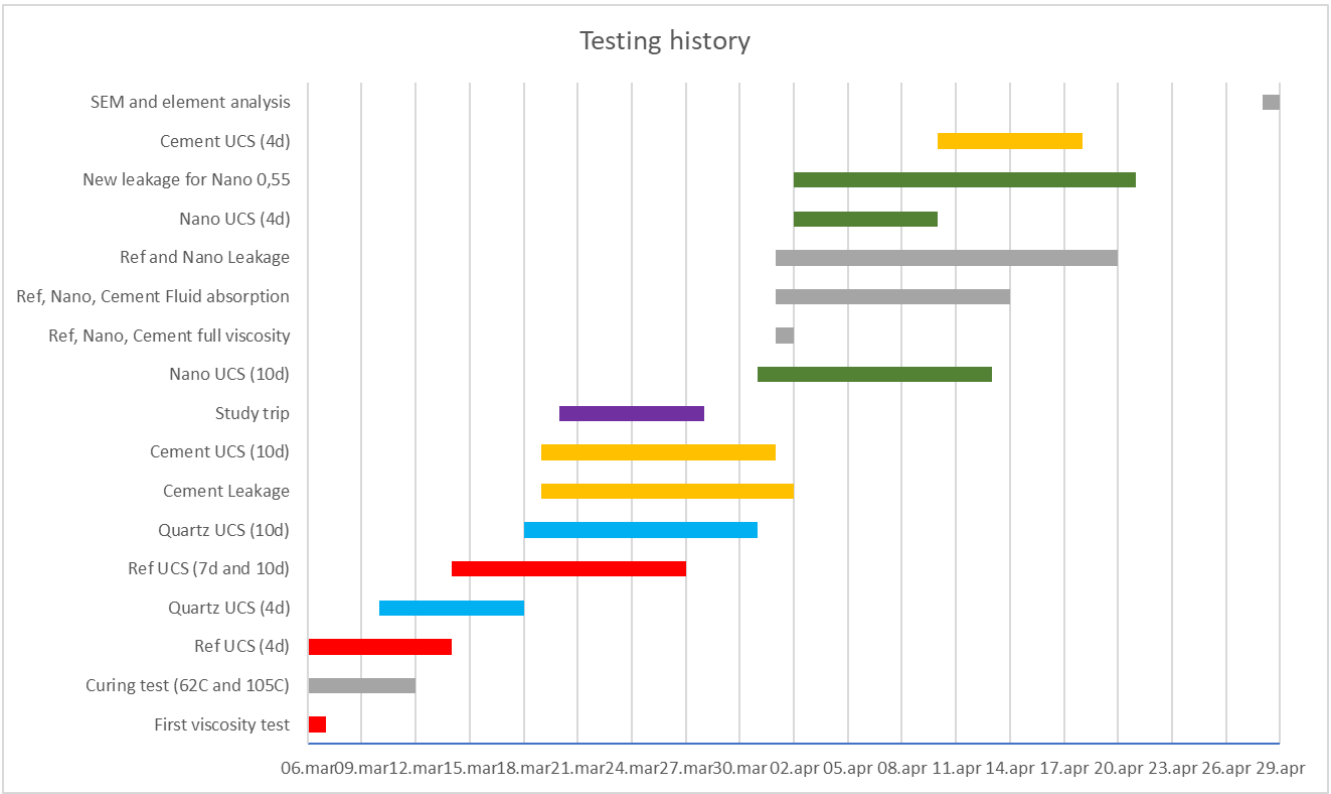

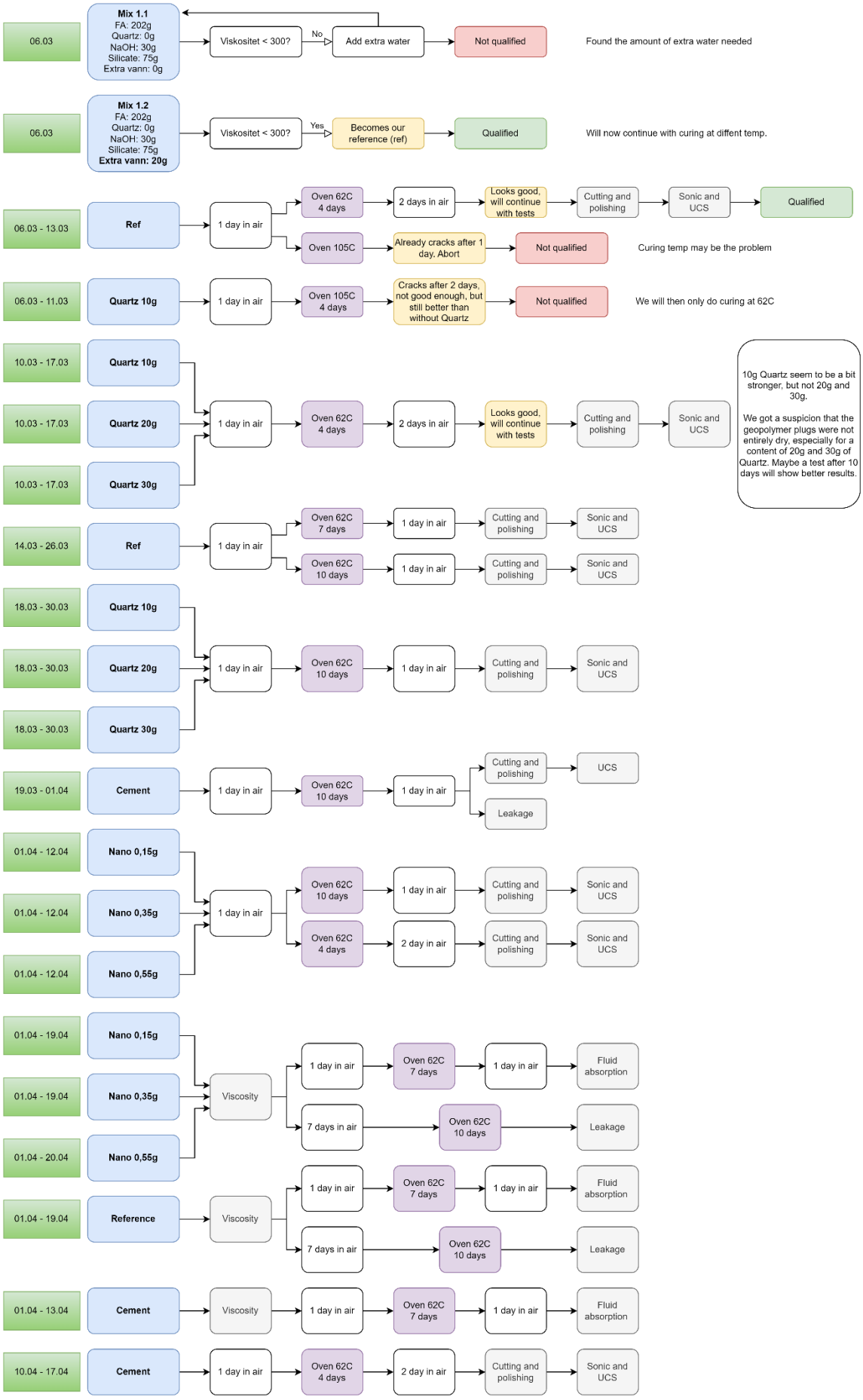
06.03
Mix 1.1
FA: 202g
Quartz: 0g
NaOH: 30g
Silicate: 75g
Extra vann: 0g
Viskositet < 300?
No
Add extra water
Not qualified
Found the amount of extra water needed
06.03
Mix 1.2
FA: 202g
Quartz: 0g
NaOH: 30g
Silicate: 75g
Extra vann: 20g
Viskositet < 300?
Yes
Becomes our reference (ref)
Qualified
Will now continue with curing at diffent temp.
06.03 - 13.03
Ref
1 day in air
Oven 62C 4 days
2 days in air
Looks good, will continue with tests
Cutting and polishing
Sonic and UCS
Qualified
Oven 105C
Already cracks after 1 day. Abort
Not qualified
Curing temp may be the problem
06.03 - 11.03
Quartz 10g
1 day in air
Oven 105C 4 days
Cracks after 2 days, not good enough, but still better than without Quartz
Not qualified
We will then only do curing at 62C
10.03 - 17.03
Quartz 10g
10.03 - 17.03
Quartz 20g
10.03 - 17.03
Quartz 30g
1 day in air
Oven 62C 4 days
2 days in air
Looks good, will continue with tests
Cutting and polishing
Sonic and UCS
10g Quartz seem to be a bit stronger, but not 20g and 30g.
We got a suspicion that the geopolymer plugs were not entirely dry, especially for a content of 20g and 30g of Quartz. Maybe a test after 10 days will show better results.
14.03 - 26.03
Ref
1 day in air
Oven 62C 7 days
1 day in air
Cutting and polishing
Sonic and UCS
Oven 62C 10 days
1 day in air
Cutting and polishing
Sonic and UCS
18.03 - 30.03
Quartz 10g
18.03 - 30.03
Quartz 20g
18.03 - 30.03
Quartz 30g
1 day in air
Oven 62C 10 days
1 day in air
Cutting and polishing
Sonic and UCS
19.03 - 01.04
Cement
1 day in air
Oven 62C 10 days
1 day in air
Cutting and polishing
UCS
Leakage
01.04 - 12.04
Nano 0,15g
01.04 - 12.04
Nano 0,35g
01.04 - 12.04
Nano 0,55g
1 day in air
Oven 62C 10 days
1 day in air
Cutting and polishing
Sonic and UCS
Oven 62C 4 days
2 day in air
Cutting and polishing
Sonic and UCS
01.04 - 19.04
Nano 0,15g
01.04 - 19.04
Nano 0,35g
01.04 - 20.04
Nano 0,55g
Viscosity
1 day in air
Oven 62C 7 days
1 day in air
Fluid absorption
7 days in air
Oven 62C 10 days
Leakage
01.04 - 19.04
Reference
Viscosity
1 day in air
Oven 62C 7 days
1 day in air
Fluid absorption
7 days in air
Oven 62C 10 days
Leakage
01.04 - 13.04
Cement
Viscosity
1 day in air
Oven 62C 7 days
1 day in air
Fluid absorption
10.04 - 17.04
Cement
1 day in air
Oven 62C 4 days
2 day in air
Cutting and polishing
Sonic and UCS

11 Appendix C – SEM Images

Geopolymer reference

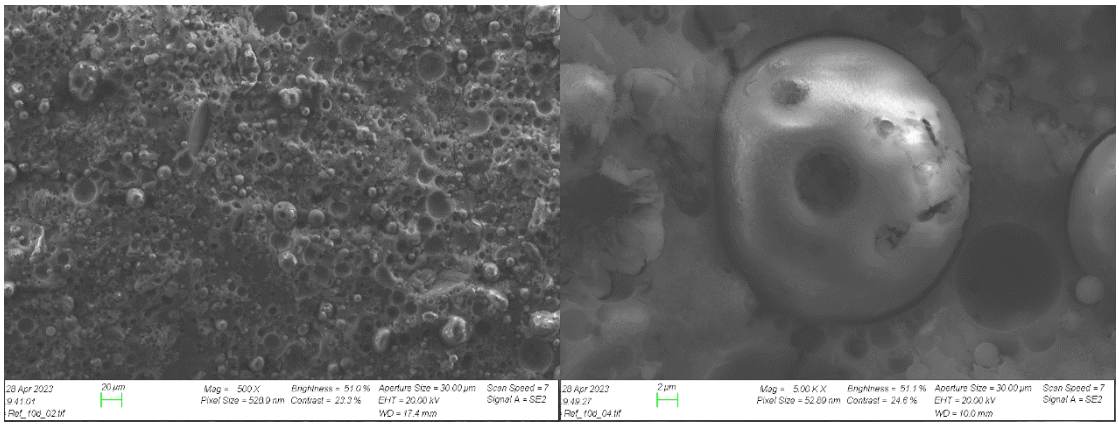

Geopolymer reference with Quartz (30g)

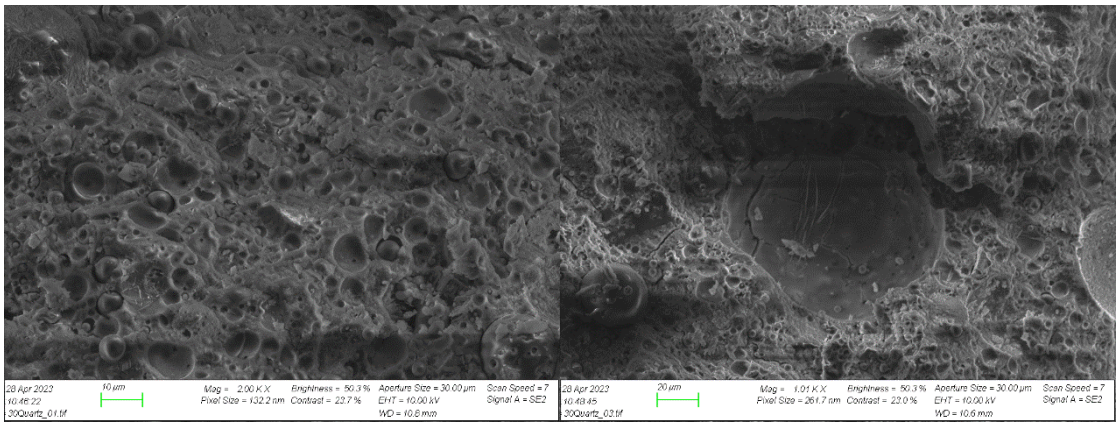

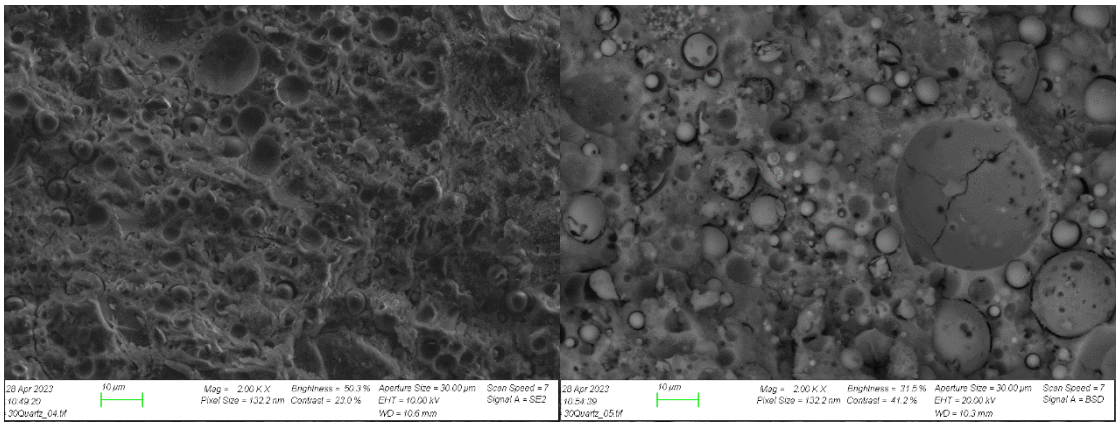

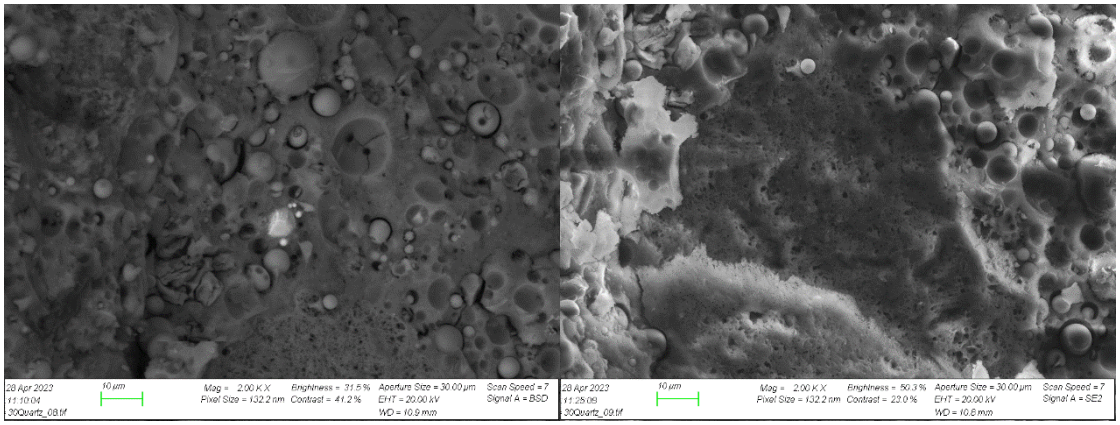

Geopolymer reference with Nano-Silica (0,55g)